UNIVERSITY OF OKLAHOMA

GRADUATE COLLEGE

EVALUATION OF METHANE-OXIDIZING BACTERIA PHYSIOLOGICAL RESPONSES TO CHANGES IN OXYGEN CONCENTRATION, INTERACTIONS WITH NON-METHANE-OXIDIZING HETEROTROPHIC BACTERIA, AND THE TAXONOMIC CLASSIFICATION OF METHYLOCYSTIS SUFLITAE SP. NOV.

A DISSERTATION

SUBMITTED TO THE GRADUATE FACULTY

in partial fulfillment of the requirements for the

Degree of

Doctor of Philosophy

By

CHRISTOPHER THOMAS GARNER

Norman, Oklahoma

2024

EVALUATION OF METHANE-OXIDIZING BACTERIA PHYSIOLOGICAL RESPONSES TO CHANGES IN OXYGEN CONCENTRATION, INTERACTIONS WITH NON-METHANE-OXIDIZING HETEROTROPHIC BACTERIA, AND THE TAXONOMIC CLASSIFICATION OF METHYLOCYSTIS SUFLITAE SP. NOV.

A DISSERTATION APPROVED FOR THE

SCHOOL OF BIOLOGICAL SCIENCES

BY THE COMMITTEE CONSISTING OF

Dr. Kara De León, Chair

Dr. Lee Krumholz

Dr. Paul Lawson

Dr. Krithivasan Sankaranarayanan

Dr. Andrew Elwood Madden

Acknowledgments

I would like to express my deepest gratitude to my supervisor, Dr. Lee Krumholz, for his unwavering support, invaluable guidance, and insightful feedback throughout the entirety of this research journey. His dedication, expertise, and encouragement have been instrumental in shaping the direction of this dissertation and fostering my growth as a researcher and he has inspired a goal to be a lifelong student of science. I pray for the privilege of having the same impact on my future students that he has had on me.

I extend my heartfelt appreciation to the members of my dissertation committee for their time, expertise, and constructive feedback. Their diverse perspectives and scholarly insights have greatly enriched the quality of this study. Further, I count myself lucky to have been taught by them and to have had the privilege of teaching alongside Drs. De León and Lawson during my graduate studies.

I am profoundly grateful to the University of Oklahoma for providing the resources and facilities necessary for conducting this research. Additionally, I would like to acknowledge the School of Biological Sciences and the Department of Microbiology and Plant Biology for fostering an intellectually stimulating environment conducive to the highest level of scholarly inquiry. If I were to do it all again, I would gladly choose the University of Oklahoma.

My sincere thanks go to all the Krumholz lab members and external collaborators for their assistance with data collection, analysis, and guidance. Their collaboration and camaraderie have made this research endeavor both rewarding and enjoyable. I especially want to thank Dr. Christopher Abin for his passionate commitment to my growth as a scientist and as a person. I'm honored to call you my friend.

As a special note regarding the contents of this dissertation, the first chapter is a published multi-author work (Garner CT, Sankaranarayanan K, Abin CA, Garner RM, Cai H, Lawson PA, et al. Methylocystis suflitae sp. nov., a novel type II methanotrophic bacterium isolated from landfill cover soil. International Journal of Systematic and Evolutionary Microbiology. 2024;74(1):006239.). A detailed overview of the author's contributions is found at the end of the chapter.

Thank you to my parents and to my sister for their unwavering encouragement. Their support has been a source of strength and motivation.

Finally, I want to thank my wife, Rosie. You have been constantly supportive, guiding, and patient during even the most challenging parts of this process. I cannot thank you enough for everything you do for our family. This could not have happened without you, and I am beyond grateful. And to Maria, who may one day read this, I love you. All this hard work was for you.

Table of Contents

List of Tables

List of Figures

Abstract

This work describes an in-depth investigation into how the methane-oxidizing bacteria (MOB) respond to changes that allow them to effectively function in their ecological role. This includes understanding their response to unfavorable oxygen concentrations, and how they respond in co-culture with other bacteria. This work also presents the characterization of a novel species of MOB; *Methylocystis suflitae* sp. nov. MOB play a crucial role in the global methane cycle, serving as significant actors in biogeochemical cycling. However, their physiological response to changing oxygen concentrations remains incompletely understood. One of the studies presented in this dissertation investigates how two MOB species, *Methylosinus trichosporium* OB3b and *Methylomonas* sp. WSC-7, respond to changing oxygen concentrations and the addition of catalase, a hydrogen peroxide scavenger, in growth media. Through transcriptomics analysis, this work showed that under high oxygen conditions, *M. trichosporium* OB3b upregulates genes involved in reactive oxygen species (ROS) defense, including cytochrome c peroxidase and superoxide dismutase, suggesting a need to deal with elevated ROS levels. Conversely, *Methylomonas* sp. WSC-7 exhibits cell clustering behavior, potentially as a defense mechanism against ROS toxicity. Differential expression of flagellar biosynthesis genes and chemotaxis response genes further supports this adaptive response. Moreover, *Methylomonas* sp. WSC-7 shows reduced expression of soluble methane monooxygenase genes under low oxygen conditions, while *M. trichosporium* OB3b exhibits higher expression under catalase-amended conditions, and that rates of methane oxidation for both strains are impacted by the concentration of oxygen and amending the growth media with catalase. Our findings underscore the importance of oxygen concentration in modulating MOB physiology and suggest potential strategies for optimizing their growth conditions. Additionally, despite the MOB's crucial role in

biogeochemical cycling, there is still a lot to learn about how the MOB interact with other bacteria in their environment. Another aspect of this study investigates the growth conditions and community dynamics of methane-oxidizing co-cultures, focusing on the interactions between *M. trichosporium* OB3b (MOB) and the non-methane-oxidizing heterotrophic bacteria (NMOHB) of the genera *Flavobacterium*, *Cupriavidus,* and *Pseudomonas*. Heterotrophic plate counts were used to determine whether NMOHB could grow in methane-oxidizing co-cultures. There was growth of all three NMOHB, suggesting carbon substrate utilization derived from methane oxidation. Furthermore, co-cultures with *Pseudomonas chlororaphis* HC exhibited enhanced methane oxidation rates compared to monoculture, indicating a stimulating effect of *P. chlororaphis* HC on methane utilization by MOB. Transcriptomic analysis revealed differential gene expression patterns in both MOB and NMOHB during co-culture and points to potential cross-feeding of C4 dicarboxylates and methanol from the MOB to the NMOHB. Further, NMOHB displayed upregulation of genes involved in ROS remediation, suggesting a response to oxidative stress induced by methane oxidation. Additionally, NMOHB exhibited alterations in nitrogen utilization and amino acid metabolism genes, possibly reflecting adaptations to the co-culture environment. Overall, these findings shed light on the metabolic interactions between MOB and NMOHB in methane-oxidizing systems, highlighting the potential for carbon sharing, nitrogen exchange, and ROS defense mechanisms.

Chapter 1

Description of *Methylocystis suflitae* sp. nov., a novel type II methanotrophic bacterium isolated from landfill cover soil.

Christopher T. Garner[1], Krithivasan Sankaranarayanan[2], Christopher A. Abin[1,2], Rosa M. Garner[1], Haiyuan Cai[3], Paul A. Lawson[1], Lee R. Krumholz[1,4]

1) Department of Microbiology and Plant Biology, University of Oklahoma, 770 Van Vleet Oval, Norman, OK, USA, 73019

2) Laboratories of Molecular Anthropology and Microbiome Research, Stephenson Research and Technology Center, University of Oklahoma, 101 David L. Boren Blvd., Norman, OK, USA, 3019

3) Nanjing Institute of Geography and Limnology, Chinese Academy of Sciences, Nanjing, China. 73 East Beijing Road, Nanjing 210008, P.R.China

4) Institute for Energy and the Environment, Mewbourne College of Earth and Energy, University of Oklahoma, Norman, OK 73019.

Abbreviations: TEM – Transmission Electron Microscopy; AAI – Average Amino Acid Identity; ANI – Average Nucleotide Identity ; dDDH - digital DNA-DNA hybridization

Repositories: This strain is in the type culture collection of the ATCC with the type culture designation TSD-256 and has been deposited in the DSMZ German Collection of Microorganisms and Cell Cultures GmbH under the number DSM 112294.

Genome GenBank Accession Number: GCA_024448135.1

16S rRNA GenBank Accession Number: ON715489

A bacterial strain designated NLS-7^T, was isolated through enrichment of landfill cover soil in methane-oxidizing conditions. Strain NLS-7^T is a Gram-stain negative, non-motile, rod approximately 0.8 μm wide by 1.3 μm long. Phylogenetic analyses based on 16S rRNA gene sequencing places it within the genus *Methylocystis*, with its closest relatives being *M. hirsuta*, *M. silviterrae*, and *M. rosea*, with 99.9%, 99.7%, and 99.6% sequence similarity respectively.

However, ANI and AAI values below the 95% threshold compared to all the close relatives with dDDH values between 20.9-54.1 demonstrate that strain NLS-7^T represents a novel species. Genome sequencing generated 4.31 million reads and genome assembly resulted in the generation of 244 contigs with a total assembly length of 3,820,957 bp (N50: 37,735 bp; L50: 34). Genome completeness is 99.5% with 3.98% contamination. It is capable of growth on methane and methanol. It grows optimally at 30 °C between pH 6.5-7.0. Strain NLS-7^T is capable of atmospheric dinitrogen fixation and can use ammonium (as NH_4Cl), L-aspartate, L-arginine, yeast extract, nitrate, L-leucine, L-proline, L-methionine, L-lysine, and L-alanine as nitrogen sources. The major fatty acids are $C_{18:1}$ ω8c and $C_{18:1}$ ω7c. Based upon this polyphasic taxonomic study, strain NLS-7^T represents a novel species of the genus *Methylocystis*, for which the name *Methylocystis suflitae* sp. nov. is proposed. The type strain is NLS-7^T (ATCC = TSD-256, DSMZ = DSM 112294). The 16S rRNA gene and genome sequences of strain NLS-7^T have been deposited in GenBank under accession numbers ON715489 and GCA_024448135.1, respectively.

Introduction

Methanotrophs are organisms that can oxidize methane as their primary carbon and energy source (1). Methane is a potent greenhouse gas (2), and these organisms play a significant role in the global methane cycle (3). Successful isolation and characterization of methanotrophs is useful in understanding their total effect on the global methane budget. Methanotrophs are highly abundant in landfill cover soils due to the high levels of methane produced in anoxic zones beneath the surface (4). Knief et. al (5) speculate that landfill cover soil hosts a diverse group of uncultivated methanotrophic species and that methanotrophs of the genus *Methylocystis* show habitat specificity for landfill cover soil.

Methylocystis is a genus of type II methanotrophs in the class *Alphaproteobacteria* within the family *Methylocystaceae*. To date, the genus encompasses eight species with validly published names. In 1993, Bowman *et al*. presented a revised methanotroph taxonomy to show the *Methylocystis* genus as containing the species *M. parva and M. echinoides* (6). Since then, six more isolates have been characterized within the genus. These include: *M. rosea* (7), *M. hirsuta* (8), *M. heyeri* (9), *M. bryophila* (10), *M. silviterrae* (11), and *M. iwaonis (12)*. The work done to characterize the *M. iwaonis* species presents the most recent emendation and description of the *Methylocystis* genus (12).

Isolation and Ecology

Methylocystis strain NLS-7^T was isolated from landfill cover soil of the United States Geological Survey Norman Landfill Environmental Research Site in Norman, Oklahoma, USA (35° 10' 12" N 97° 26' 49" W). The soil sample was obtained at a depth of 2-4 cm. Enrichments were made by incubating 5 g of soil in 120 mL serum bottles fitted with butyl rubber stoppers at 26 °C and amended with methane at 1% of the headspace volume. Methane oxidation was monitored by gas chromatography on a Shimadzu GC-14A gas chromatograph (Shimadzu, Japan). Following depletion of methane, enrichment cultures were reamended three times. Following this initial enrichment, a ten-fold dilution series was prepared to further enrich the most abundant methanotrophs present in the soil. The dilution series was performed in triplicate using 10 mL of modified NMS medium in 28 mL serum tubes amended with methane at 0.2% of the tube's headspace. The modified nitrate mineral salts (NMS) medium contains (per liter of distilled water) 1 g KNO_3, 0.27 g KH_2PO_4, 1 g $MgSO_4 \cdot 7H_2O$, 0.14 g $CaCl_2 \cdot 2H_2O$, and 0.23 g Na_2HPO_4, 0.5% (v/v) acidic trace element solution (AcTES), 0.02% alkaline trace element solution (AlTES), and 1% vitamin solution. AcTES contains (per liter), 2 g $FeSO_4 \cdot 7H_2O$, 0.07

g $ZnSO_4 \cdot 7H_2O$, 0.5 g $MnCl_2 \cdot 4H_2O$, 0.12 g $CoCl_2 \cdot 6H_2O$, 0.01 g $NiCl_2 \cdot 6H_2O$, 0.5 g $CuSO_4$, 0.01 g H_3BO_3, 0.06 g $LaNO_3$, 0.06 g $CeNO_3$, and 100 mM HCl. The AlTES contains (per liter) 0.11 g Na_2SeO_4, 0.05 g Na_2WO_4, 0.29 g Na_2MoO_4, and 0.04 g NaOH. The vitamin solution contains (per liter) 5 mg 4-aminobenzoic acid, 2 mg D-biotin, 2 mg folic Acid, 10 mg pyridoxine-HCl, 5 mg riboflavin, 5 mg thiamine-HCl x $2H_2O$, 5 mg nicotinic acid, 5 mg calcium D-pantothenate, 5 mg thioctic acid (α-Lipoic Acid), and 0.10 mg vitamin B12.

Methane oxidation was again measured via gas chromatography. Dilutions that showed methane oxidation were reamended with methane following depletion and the process was repeated twice. These cultures were diluted and then plated onto solid modified NMS media containing 2% agar. Petri plates were incubated in airtight ammunition boxes (normally used for storing firearm ammunition) fitted with a rubber stopper through a drilled bore hole. Methane was added to the headspace of the ammunition box at 5% of the box's interior volume. Colonies that formed on the plates were passaged on solid media up to five times until a pure colony of a single bacterial strain was present. The isolated strain was characterized and maintained in liquid modified NMS media in 160 mL serum bottles with methane added at 1-10% of the bottle's headspace.

Genome Features and Phylogeny

Genomic DNA was extracted from a log-phase culture of strain NLS-7^T grown in the modified NMS medium at 28°C using the Qiagen DNeasy Blood and Tissue Kit according to the manufacturer's instructions. Genomic DNA was fragmented using a QSonica 800R3 sonicator and built into Illumina-compatible shotgun libraries using the KAPA HyperPrep Kit following the manufacturer's protocol. Shotgun libraries were sequenced on an Illumina MiSeq instrument. Sequence data was processed using fastp (v0.23.2) to remove reads containing uncalled bases

('N'), trim low-quality bases (q < 30), and merge overlapping reads (13). The resulting analysis-ready reads were used as input for *de novo* assembly (SKESA v2.5.1) (14). The quality of genomes was assessed by CheckM (v1.1.3) (15).

Reference genome sequences were obtained for representative bacterial species in the family *Methylocystaceae* (*Methylocystis*, *Methylophila*, *Chenggangzhangella,* and *Hansschlegelia*) from the NCBI RefSeq and GenBank databases (16,17). Gene prediction was performed using Prodigal (mRNA, v2.6.3), Barrnap (rRNA, v0.9) and tRNAscan-SE (tRNA, v2.0.9) (18). Annotation of protein-coding genes was performed using the KEGG database as reference (BLASTP, KoFamScan) (19–21). Predicted proteins were used to generate pairwise Average Amino Acid Identity scores (AAI, Enveomics toolbox) for genome-based taxonomic delineation (22). Average Nucleotide Identity (ANI) scores were calculated using the fastANI algorithm (23).Finally, sequences for 92 single-copy core bacterial genes were retrieved using the UBCG pipeline, aligned (MUSCLE), filtered to remove invariant sites, and concatenated (24,25). This concatenated sequence set was used to construct a maximum-likelihood amino acid tree (RAxML, 100 bootstrap replicates, GTR substitution model) to characterize the phylogenetic relationship between strain NLS-7^T and other representatives of the family *Methylocystaceae* (26).

A total of 4.31 million reads (1.17 million merged, 0.98 million paired) were generated following quality filtering. Genome assembly resulted in the generation of 244 contigs with a total assembly length of 3,820,957 bp (N50: 37,735 bp; L50: 34). A total of 3,938 protein-coding, 46 tRNA, and three rRNA genes were identified. Genome completion was estimated at 99.5% based on the recovery of 1,095 single-copy genes (total 1,100) found in representative genomes of members of the *Methylocystis* genus. Genome contamination is 3.98% (15). Of the 3,938

predicted proteins, 2,957 were assigned function, 662 were hypothetical or had unknown function, and 319 had no significant matches.

Comparisons of the 16S rRNA gene sequence for strain NLS-7^T with other validly published species of the genus *Methylocystis* were performed by aligning complete 16S rRNA sequences (1,497bp) using MUSCLE (25), followed by estimation of pairwise sequence similarities using NCBI's blastn tool (20). Strain NLS-7^T shares 99.9%, 99.7%, and 99.6% sequence similarity with *M. hirsuta*, *M. silviterrae*, and *M. rosea*, respectively (**Supplemental Table 1**). A partial 16S rRNA sequence of strain NLS-7^T was also obtained by single gene PCR amplification and Sanger sequencing (Oklahoma Medical Research Foundation, Oklahoma City, USA). The primer set used for the single gene amplification was the 27F (5'-AGAGTTTGATCMTGGCTCAG-3') and 1492R (5'-TACGGYTACCTTGTTACGACTT-3') (27)**.** This partial region matches the 16S rRNA gene from the whole genome sequence. Genome-wide estimates of similarity (ANI, AAI and dDDH, **Table 1**) also show that strain NLS-7^T is most closely related to *M. silviterrae* (93.03% ANI, 93.86% AAI, 53.7% dDDH), *M. hirsuta* (92.63% ANI, 93.65% AAI, 54.1% dDDH), and *M. rosea* (91.52% ANI, 92.04% AAI 46.1 % dDDH). These ANI and AAI values are below the 95% threshold used to delineate microbial species, and dDDH is less than 70% ranging from 20.9%-54.1% (**Table 1**). This indicates that strain NLS-7^T is a novel species in the *Methylocystis* genus (28–30). The multi-gene UBCG phylogenetic tree (**Figure 1**) shows that strain NLS-7^T forms a robust cluster with *M. silviterrae*, *M. hirsuta*, and *M. rosea* and is distinct from *M. parva, M. heyeri*, and *M. bryophila* (**Figure 1**). To further show the phylogenetic relationship between strain NLS-7^T and other relatives of the family *Methylocystaceae*, phylogenetic trees were constructed based on nucleotide and conserved deduced amino acid sequences of genes (*pmoA*) encoding alpha subunit of particulate methane monooxygenase

(**Figure 2**). The *pmoA* gene is commonly used for ecological studies of methanotrophic bacteria (5,31). This was done by extracting the *pmoA* gene nucleotide sequences from the NCBI reference genomes (16) by annotation with prokka (v 1.14.6) (32) and then the tree was constructed using FastTree (v2.1) (33).

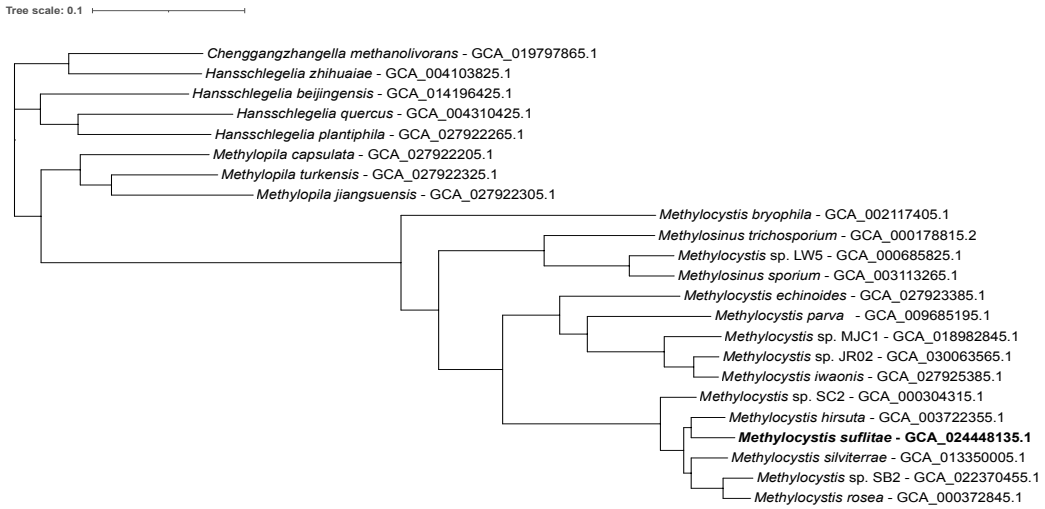

Figure 1: Phylogenetic relationship between strain NLS-7^T and representatives for members of the family Methylocystaceae. Maximum-likelihood phylogenetic tree constructed from a concatenated alignment of 92 single copy genes.

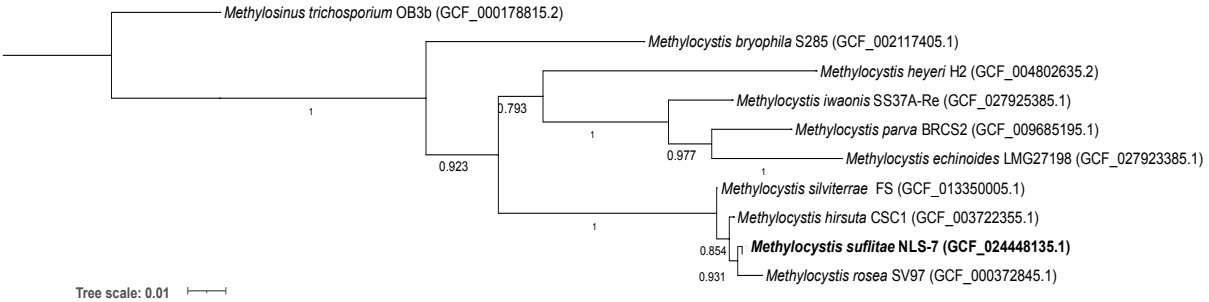

Figure 2: Phylogenetic tree based on *pmoA* gene nucleotide sequence phylogeny for classified *Methylocystis* species and *Methylosinus trichosporium* OB3b. The phylogeny was computed by FastTree 2.1's Heuristic Neighbor-Joining method with a GTR substitution model and 1,000 resamples (32). Branch lengths numbers represent the proportion of resamples that fitted to that branch length.

Table 1: Comparative ANI, AAI, and dDDH values for characterized strains of species in the genus *Methylocystis* against strain NLS-7^T. All ANI and AAI values are less than 95% and all dDDH values are less than 70% demonstrating species level delineation of strain NLS-7^T.

Organism Name	**GenBank ID**	**ANI**	**AAI**	**dDDH**
M. bryophila	GCF_002117405.1	78.41	64.60	20.9
M. echinoides	GCF_027923385.1	79.89	70.89	22.1
M. parva	GCF_009685195.1	79.71	72.05	22.0
M. iwaonis	GCF_027925385.1	79.80	71.98	22.0
M. rosea	GCF_000372845.1	92.04	91.53	46.1
M. heyeri	GCF_004802635.2	78.41	66.45	20.9
M. hirsuta	GCF_003722355.1	93.65	92.63	54.1
M. silviterrae	GCF_013350005.1	93.86	93.03	53.7

A search for common chemotaxonomic markers (membrane polar lipids, peptidoglycan diagnostic diamino acids) identified cardiolipin synthase (EC: 2.7.8.41, K08744), CDP-diacylglycerol---serine O-phosphatidyltransferase (EC:2.7.8.8, K17103), phosphatidylserine decarboxylase (EC:4.1.1.65, K01613), and the murE ligase (EC:6.3.2.13, K01928), associated with the biosynthesis of diphosphatidylglycerol (DPG, cardiolipin), phosphatidylserine (PS), phosphatidylenthanolamine (PE), and the diagnostic diamino acid meso-diaminopimelic acid (m-

DPM), respectively(34,35). These genes were observed in the genomes of all *Methylocystis* species (including isolate NLS-7^T).

The genetic relationship between strain NLS-7^T and related species of the genus *Methylocystis* was further studied by determining the pan-genome of *Methylocystis* using the pan-genome workflow of Anvi'o v7 (36). The program “anvi-gen-contigs-database” was first used to profile genomes of the genus *Methylocystis,* during which Prodigal v2.6.3 with default settings identified open reading frames (37). The program 'anvi-run-kegg-kofams' was used to annotate genes with functions by searching them against the latest KEGG database using blastp (20). The program 'anvi-pan-genome' with the flag ‘--use-ncbi-blast’, and parameters ‘--minbit 0.5′, and ‘--mcl-inflation 8′ was used to run the pan-genomic analysis. This program calculates similarities of each amino acid sequence in every genome against every other amino acid sequence in the group of genomes using blastp (20) and uses the MCL algorithm to identify gene clusters (38). The flag "anvi-display-pan" was used to visualize the distribution of gene clusters across genomes. In total, 508 gene clusters were identified that are unique to strain NLS-7^T within the genus *Methylocystis*. This work further supplements our genomic analysis described above, demonstrating that with ortholog clustering and unique gene cluster determination, the proportion of genes unique to NLS-7^T is similar to the proportion of unique genes found in other species of *Methylocystis*, especially *M. rosea* and *M. silviterrae* (**Figure 3, Supplemental Table 2, Supplemental Table 3)**. *M. silviterrae* has 334 unique gene clusters, and *M. rosea* has 436 unique gene clusters. *M. echinoides* has the most gene clusters unique to its genome with 1629 clusters followed by *M. heyeri* with 1226 and *M. broyophila* with 1149. The species with high numbers of unique gene clusters in their genome also have AAI values that are low (<77%) compared to every other species in the genus *Methylocystis* (**Supplemental Table 4**). Strains that

don’t have as many unique gene clusters have relatively higher AAI values in pairwise comparison (**Supplemental Table 4**). A portion of the genes unique to strain NLS-7^{T} were annotated to be in the coenzyme transport and metabolism, cell wall/membrane/envelope biogenesis, carbohydrate transport and metabolism, and amino acid transport and metabolism COG20 annotation categories (39) though most were unknown or unannotated (**Supplemental Table 3**).

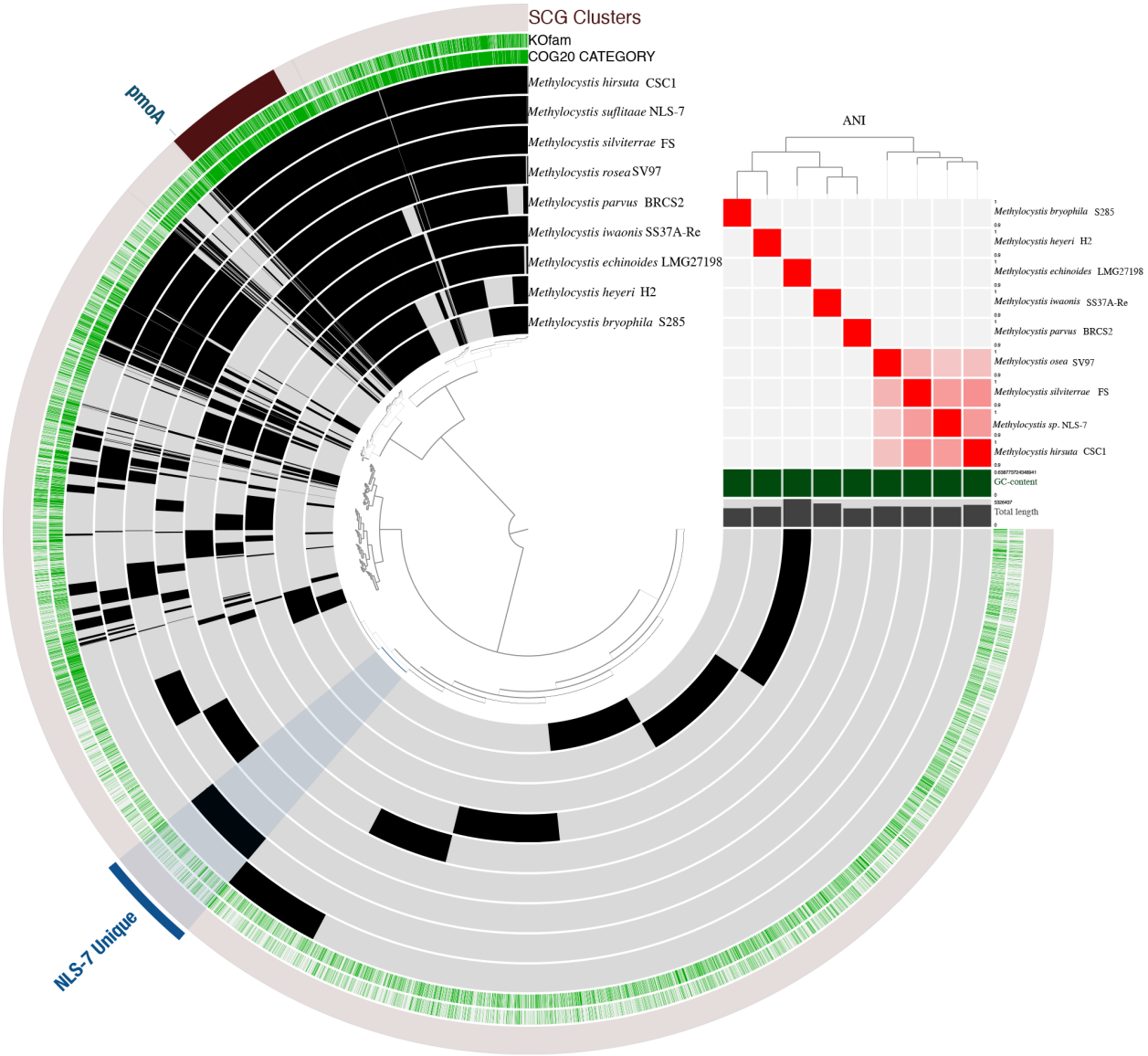

Figure 3: The pangenome of the genus Methylocystis as determined by the Anvi'o workflow [36]. Overlapping black boxes represent portions of the genome that are shared by any two or more species, while segments of the genome that are unique to a certain species do not overlap with another.

Figure 3: Pangenome of *Methylocystis* – Unique Genes

Physiology and Chemotaxonomy

Cells for microscopy were grown to mid log-phase in the modified NMS medium in air with 10% CH_4 as the carbon and energy source. All the following growth experiments were at 28 °C unless otherwise indicated. Cell size estimates, motility, and morphological descriptions of strain NLS-7^T were determined through light microscopy of wet mounts of cells grown in liquid culture using an Olympus BX41 microscope (Olympus Corporation, Japan) fitted with a Jenoptik Gryphax Subra camera and PROGRES GRYPHAX imaging software v 2.0.0.66 (Jenoptik Group, Germany). Cells for transmission electron microscopy were grown to mid log phase, harvested by centrifugation, and resuspended in 1% molten agarose. After cooling, the agarose was cut into blocks and pre-fixed with 4% (w/v) glutaraldehyde in 0.2 M cacodylate buffer (pH 7.4) for 1 h at room temperature and then overnight at 4 °C. Cells were then rinsed with 3 changes of cold 0.2 M cacodylate buffer for 10 minutes each and fixed in 2% OsO_4 for 2 hours on ice. Blocks were then rinsed in cold buffer and stored overnight at 4 °C. They were dehydrated in an ethanol series followed by a propylene oxide substitution and embedded in a Spurr epoxy resin. Resin blocks were thin sectioned using an Ultramicrotome (Reichert-Jung Ultracut E). Thin sections (50-70 nm) were collected on formovar-coated size 300 mesh copper

grids and stained with 2% uranyl acetate and 2% lead citrate for 10 minutes each. Thin sections were imaged at 80 kV on a JEOL 2010F TEM, equipped with a cold field emission electron source and a Direct Electron DE-12 (4k x 3k) digital imaging system. TEM imaging was performed at the Oklahoma Medical Research Foundation (Oklahoma City, USA).

Cell growth was measured for carbon and nitrogen source utilization tests, NaCl concentration tolerance, and temperature and pH range by analyzing the OD_{600} of cultures with a Thermo Spectronic 20 D+ spectrophotometer (Thermo Scientific, USA) in the above medium.

Temperature range was determined by measuring growth rates at 4, 15, 20, 25, 30, 35, 40, and 45 °C. The pH range was examined from 5.0–9.0 in 0.5 pH increments and NaCl tolerance measured at concentrations of 0–2% (w/v) in 0.25% increments. To determine substrate utilization abilities of the strain, the following carbon sources were individually added to the modified NMS media at 0.1% w/v: methanol, ethanol, formate, glucose, fructose, lactose, sucrose, maltose, xylose, sorbitol, alanine, serine, glycine, acetate, citrate, oxalate, malate, pyruvate, succinate, urea, methylamine, dimethylamine, dimethylcarbonate, formamide, and methane (10% of tube headspace). Formaldehyde was also tested as a growth substrate, but at 0.01% w/v to compensate for potential toxicity issues and growth was measured using direct cell counts with 0.01% acridine orange stained cells and fluorescence microscopy (40)**.** Cells were counted using the Olympus BX41 microscope described above fitted for fluorescence emission at 480 nm (Olympus Corporation, Japan). For all carbon source utilization experiments, growth was measured weekly for 6 weeks. Nitrogen source utilization was tested by adding at 0.1% w/v, the following nitrogen sources to a nitrate free modified NMS medium in tubes containing air and CH_4 in a 90:10 ratio in the headspace. Nitrogen sources included ammonium (as NH_4Cl), formamide, methylamine, glycine, hydroxylamine, urea, L-serine, L-aspartate, L-arginine, L-

leucine, L-proline, L-cysteine, L-methionine, L-histidine, L-lysine, L-alanine, L-threonine, glutamine, yeast extract, and nitrite. Each of these nitrogen sources were compared to a no added fixed nitrogen source control. Growth was measured every 1-2 weeks for 5-6 weeks. To determine if strain NLS-7^T was able to fix atmospheric N_2, it was grown in a nitrogen free medium with N_2, O_2, and CH_4 gases present in the headspace at a 70:20:10 ratio and compared to a control with He substituted for N_2. This control therefore has a headspace gas composition of He, O_2, and CH_4 at the sample 70:20:10 ratio. Growth was measured weekly for 8 weeks.

Strain NLS-7^T was capable of growth solely on methane and methanol. It was able to utilize ammonium (as NH_4Cl), L-aspartate, L-arginine, yeast extract, Nitrate, L-leucine, L-proline, L-methionine, L-lysine, and L-alanine as nitrogen sources. Like all other members of the genus *Methylocystis*, strain NLS-7^T can fix atmospheric N_2. Strain NLS-7^T can tolerate up to 0.75% (w/v) NaCl. It grew between 10-35 °C with an optimum at 30 °C and grew from pH 5.5-8.5 with an optimal pH of 6.5-7.0. When growing at 30 °C and pH 6.8 the strain has a specific growth rate of approximately 0.06 h^{-1}. Cells are Gram-stain negative rods and are approximately 0.8 ± 0.14 µm wide by 1.3 ± 0.3 µm long (**Figure 4a**) when observed by light microscopy. When examining thin sections of the cells with transmission electron microscopy, there appears to be accumulation of poly-β-hydroxybutyrate and the cells appear to have a dumbbell shape.(**Figure 4b and 4c**).

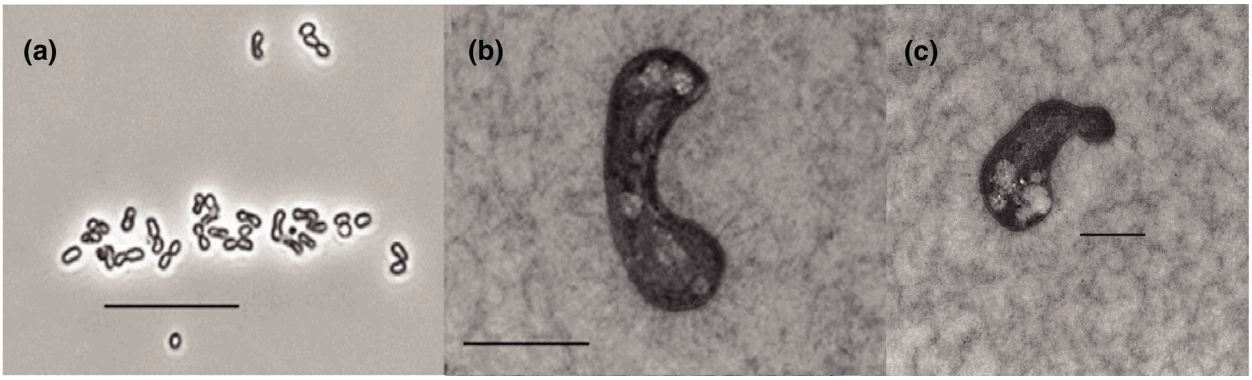

Figure 4: Microscope images of strain NLS-7. Light microscope image under a X100 oil immersion lens (a). Scale bar is 5 µm. Transmission electron microscope images (b, c). High voltage is 80 kV and direct magnification is 5000x. Scale bars are 500 nm.

Cells for fatty acid analysis were grown in modified NMS medium at 26 °C, harvested in late log phase from batch culture and the cell material was freeze dried. Phospholipid fatty acid analysis with mass spectrometry of strain NLS-7^T was carried out by the Identification Service, Leibniz-Institut – Deutsche Sammlung von Mikroorganismen und Zellkulturen GmbH, Braunshweig, Germany.

Fatty acid analysis indicates that strain NLS-7^T contains the $C_{18:1}$ ω8c, $C_{18:1}$ ω7c as the predominant fatty acids. The $C_{18:1}$ ω8c fatty acid is present in all classified members of the *Methylocystis* genus, and the $C_{18:1}$ ω7c fatty acid is present in all species of *Methylocystis* except for *M. iwaonis* (12) as shown in **Table 2**. For strain NLS-7^T, the $C_{18:1}$ ω8c and $C_{18:1}$ ω7c fatty acids are present at the highest abundance at over 97% of the entire fatty acid profile with all

other fatty acids present only at trace amounts. Although not grow all nine of the species were grown in parallel, very similar growth conditions were used to grow NLS-7^T cells as were used for the other data. Specifically the data from the characterization of *M. iwaonis* which grew cells for fatty acid analysis in NMS medium at 30°C (12).

Based on the data obtained from this polyphasic taxonomic study that included phenotypic and phylogenetic information, strain NLS-7^T merits recognition as representing a novel species of the genus *Methylocystis* for which the name *Methylocystis suflitae* sp. nov. is proposed. The novel species can be delineated from other members of the genus *Methylocystis* based on its ANI and AAI values, digital DNA-DNA hybridization, and proportion of gene clusters unique to the species. It can also be distinguished from other species of *Methylocystis* (except *M. silviterrae*) by its low diversity of fatty acids that comprise >1% of the fatty acid profile (**Table 2**). Additionally, it can be distinguished from its nearest neighbors (*M. silviterrae, M. hirsuta* and *M. rosea*) by other means. Compared to *M. silviterrae*, strain NLS-7^T can be observed to have a dumbbell shape (using transmission electron microscopy) and is shorter. The shortest *M. silviterrae* cells are reported to be longer than the average NLS-7T cell. Also, *M. silviterrae* has been shown to grow at 4 °C while NLS-7^T cannot. Strain NLS-7^T can be distinguished from *M. hirsuta* by NLS-7^T's inability to grow on acetate, and its lack of sMMO. Strain NLS-7^T can be distinguished from *M. rosea* by *M. rosea's* ability to form pink colored colonies. The strain's cellular and physiological characteristics are detailed and summarized in **Table 3**.

Table 2: Fatty acid profile of strain NLS-7^T compared to other members of the genus *Methylocystis*. Numbers represent the relative percentage of the acid. The comparative strains are: 1. *M. heyeri*; 2. *M. rosea;* 3. *M. echinoides*; 4. *M. parva*; 5. *M. hirsuta*; 6. *M. bryophila*; 7. *M. silviterrae* ; 8. *M. iwaonis*. The data for strain NLS-7^T were obtained in this study with the rest of the data obtained in the work describing the characterization of *M. iwanois* (12). Trace fatty acids comprising <1% of the total profile are not presented and shown as a dash.

Fatty acid	*M. suflitae* NLS-7^T	1	2	3	4	5	6	7	8
10-Methyl $C_{16:0}$	-	3.5	-	-	-	-	-	-	-
$C_{16:1}\omega 8c$	-	29.0	-	-	-	-	-	-	-
$C_{16:1}\omega 7c$	-	3.4	6.1	-	-	-	15.4	-	1.2
$C_{16:1}\omega 5t$	-	2.8	-	-	-	-	-	-	-
$C_{16:0}$	-	1.2	-	-	-	-	2.4	-	4.7
$C18:1\omega 9t$	-	14.7	-	1.5	-	-	-	-	-
$C_{18:1}\omega 8t$	-	-	-	-	-	1.5	-	-	51.8
$C_{18:1}\omega 9c$	-	-	-	-	-	-	-	-	-
$C_{18:1}\omega 8c$	69.2	32.0	74.8	51.9	45.5	71.1	53.1	74.5	27.3
$C_{18:1}\omega 7c$	28.3	10.9	23.7	18.1	23.7	26.1	19.3	24.7	-
$C_{18:0}$	-	0.7	-	-	-	-	-	-	1.4
$C_{18:2}\omega 7,12c$	-	-	-	22.7	8.0	-	7.8	-	
$C_{18:2}\omega 6,12c$	-	-	-	4.4	22.1	-	-		

Table 3: Compilation of the characterizing features of the genus *Methylocystis*. Reference strains: 1. *M. bryophila;* 2. *M. heyeri*; 3, *M. rosea*; 4. *M. echinoides;* 5. *M. parva;* 6. *M. hirsuta;* 7. *M. silviterrae;* 8. *M. iwanois.* ND, No data available; W, weakly positive.

Characteristic	*M. suflitae* NLS-7^T	1	2	3	4	5	6	7	8

Cell shape	Rods, dumbbells	Small, curved coccoids, short rods	Straight, polymorphic or regularly curved rod, ovoids	Rods	Coccobacilli, rods	Rods, coccobacilli	Dumbbell	Small curved coccoids/rods	Rods
Cell width (μm)	0.8	0.9–1.4	0.8–1.2	0.8–1.1	0.6	0.5–0.8	0.3–0.6	0.5-0.7	1.1
Cell length (μm)	1.3	1.8–3.4	1.4–4.0	1.1–2.5	0.8–1.2	1.0–2.0	0.7–1.0	1.7-3.4	2.7
Color of colonies	Yellow	Light cream	White	Pink–red	White, buff, pale pink	Diffusible brown, pale pink	Cream	Cream	White
Temperature for growth (°C)									
Optimum	30	25–30	25	27	27–30	28–30	30	4-37	25-30
Range	10-35	8–37	5–30	5–37	15–30	15–37	ND	25-30	15-37
pH for growth									
Range	5.5-8.5	4.2–7.5	4.4–7.5	5.0-9.0	5.5–8.5	5.0–9.0	ND	4.5-7.5	6.0-9.0
Optimum	6.5-7.0	6.0–6.5	5.8–6.2	ND	6.5–7.5	6.5–7.5	7.0	6.0-6.5	7.0-8.0
Growth on methanol (%)	+	≤0.15	≤1	–	0.2	0.1–0.3	+	+	+
Growth on acetate	-	+	W	-	W	-	W	-	-
sMMO	-	+	+	-	-	-	+	-	+
Major quinone	Not Determined	Q-8	Q-8	ND	Q-8	Q-8	Q-8	Q-8	Q-8
Presence of $C_{18:2}\omega7,12c$	-	+	-	-	+	+	+	-	-
DNA G+C content (mol%)	62.5	62.3	61.5–62.1	62	62	64–67	ND	62.6	62-64

Description of *Methylocystis suflitae*

Methylocystis suflitae (suf.li'tae. N.L. gen. n. *suflitae*) was named to honor Joseph M. Suflita, a contemporary American microbiologist, for his pioneering work in understanding biodegradation at the United States Geological Survey Norman Landfill Environmental Research Site. It is a member of the type II *Alphaproteobacterial* methanotrophic genus *Methylocystis*. It is a Gram-negative, non-motile, rod approximately 0.8 μm wide by 1.3 μm long. When growing on solid media in the presence of methane, it is yellow, circular, and convex with an entire margin and has a diameter of approximately 3 mm. It is capable of growth on methane and methanol. It grows optimally at 30 °C but can tolerate temperatures between 10-35 °C. It also grows optimally between pH 6.5-7.0 but can tolerate pH values between 5.5-8.5. Strain NLS-7^T tolerates NaCl concentrations up to 0.75% (w/v). Strain NLS-7^T is capable of atmospheric dinitrogen fixation and can use ammonium (as NH_4Cl), L-aspartate, L-arginine, yeast extract, nitrate, L-leucine, L-proline, L-methionine, L-lysine, and L-alanine as nitrogen sources. The major fatty acids are C18 : 1 ω8c, C18 : 1 ω7c. The type strain is NLS-7^T (= ATCC TSD-256 = DSM 112294). The 16S rRNA gene and genome sequences of strain NLS-7^T have been deposited in GenBank under accession numbers ON715489 and GCA_024448135.1, respectively.

Funding information

This work was supported by the National Science Foundation grant No. 1 736 255 under a subcontract from South Dakota School of Mines and Technology through the EPSCoR RII Track-2 FEC program.

Acknowledgments

We would like to thank Rajesh Sani, Venkata Gadhamshetty, Saurabh Dhiman, Robin Gerlach, Roland Hatzenpichler, Ross Carlson, Connie Chang, Matthew Fields, Ellen Lauchnor, Brent Peyton, Andrew Elwood Madden, Joi Trammell, Ravi Manjhi and Chuang Li for helpful discussions and suggestions. We would also like to acknowledge the Oklahoma Medical Research Foundation for TEM imaging, and Ralph Tanner and Neil Wofford for provision of reagents and equipment.

Author contributions

Conceptualization of ideas related to overarching research goals and aims was done by C.T.G. and L.R.K. Biochemical and physiological data were curated, maintained, and formally analysed by C.T.G. and genomic and phylogenetic data were curated, maintained and formally analysed by C.T.G. and H.C. Development and design of methodology was performed by C.T.G., L.R.K., C.A.A., K.S., H.C. and P.A.L. Research and investigation was conducted by C.T.G., R.M.G., C.A.A., K.S. and P.A.L. Management and coordination for the research activities was done by L.R.K. Oversight and leadership responsibility for research activity and execution including mentorship external to the core team was done by L.R.K. and C.A.A. Provision of study materials, reagents, materials, laboratory samples, instrumentation, computing resources and other analysis tools were provided by L.R.K., P.A.L., K.S. and the Oklahoma Medical Research

Foundation. Verification of replication and reproducibility of the experiments and results was done by L.R.K., C.A.A., K.S. and P.A.L. Preparation, creation, and presentation of the published work, specifically with visualization and data, was done by C.T.G., L.R.K., K.S., H.C. and P.A.L. Writing and preparation of the original draft was done by C.T.G., L.R.K., K.S., H.C. and R.M.G. Writing, including review, editing and critical commentary and revision was done by C.T.G., L.R.K., K.S. and P.A.L.

Supplement to Chapter 1

Supplemental Table 1: 16S sequence identity based on NCBI's blastn pairwise comparison of genome extracted 16S rRNA genes for each member of the genus *Methylocystis* and strain NLS-7^T. Percentages above 98% are bolded.

Species	[1]	[2]	[3]	[4]	[5]	[6]	[7]	[8]	[9]
M. bryophila S285 [1]	**100**	97.71	97.51	97.31	97.44	97.78	97.24	97.64	97.37
M. echinoides LMG27198 [2]	97.71	**100**	97.24	97.91	**98.31**	**99.19**	97.57	**98.25**	97.98
M. heyeri H2 [3]	97.51	97.24	**100**	97.78	96.49	97.17	97.71	97.57	97.84
M. hirsuta CSC1 [4]	97.31	97.91	97.78	**100**	96.83	97.64	**99.53**	**99.66**	**99.93**
M. iwaonis SS37A-Re [5]	97.44	**98.31**	96.49	96.83	**100**	**98.92**	96.49	97.17	96.90
M.s parva BRCS2 [6]	97.78	99.19	97.17	97.64	**98.92**	**100**	97.30	97.98	97.71
M. rosea SV97 [7]	97.24	97.57	97.71	**99.53**	96.49	97.30	**100**	**99.33**	**99.60**
M. silviterrae FS [8]	97.64	**98.25**	97.57	**99.66**	97.17	97.98	**99.33**	**100**	**99.73**
M. suflitae NLS-7 [9]	97.37	97.98	97.84	**99.93**	96.90	97.71	**99.60**	**99.73**	**100**

Supplemental Table 2: Total number of gene clusters unique to each species of the genus *Methylocystis*. Genomic analysis done on the NCBI reference genome of each species.

Species (NCBI Reference Genome)	**Number of Unique Clusters**
Methylocystis broyophila	1149
Methylocystis echinoides	1629
Methylocystis heyeri	1226
Methylocystis hirsuta	657
Methylocystis iwaonis	978
Methylocystis rosea	463
Methylocystis parva	646
Methylocystis silviterrae	334
Methylocystis suflitae NLS-7	508

Supplemental Table 3: COG20 functional annotation of genes clusters among genes that are unique to *Methylocystis suflitae* strain NLS-7 within the genus *Methylocystis*.

COG20 Annotation Categrory	**Number of Gene Clusters**
Amino acid transport and metabolism	5
Carbohydrate transport and metabolism	3
Cell Cycle Control	4
Cell wall/membrane/envelope biogenesis	14
Coenzyme transport and metabolism	10
Defense mechanisms	9
Energy production and conversion	5
Inorganic ion transport and metabolism	6
General function prediction	10
Lipid transport and metabolism	4
Mobilome: prophages, transposons	32
Posttranslational modification, protein turnover, chaperones	4
Replication, recombination and repair	24

Secondary metabolites biosynthesis, transport and catabolism	2
Signal transduction mechanisms	6
Transcription/Translation	13
Unknown/Unannotated Function	357

Supplemental Table 4: DDH values calculated by Formula 2 of the DSMZ Genome-to-Genome Distance Calculator 3.0 (37,38). This demonstrates that the DDH value of strain NLS-7 is < 70% compared to each unique species of *Methylocystis* (Reference). Each reference genome shown and corresponding data are being compared to strain NLS-7.

NCBI Reference genome	**DDH**	**Model C.I.**	**Prob. DDH is >= 70%**
Methylocystis echinoides	22.1	[19.9 - 24.6%]	0
Methylocystis iwaonis	22	[19.7 - 24.4%]	0
Methylocystis broyophila	20.9	[18.7 - 23.3%]	0
Methylocystis heyeri	20.9	[18.7 - 23.4%]	0
Methylocystis hirsuta	54.1	[51.4 - 56.8%]	32.02
Methylocystis parva	22	[19.7 - 24.4%]	0
Methylocystis rosea	46.1	[43.5 - 48.7%]	10.11
Methylocystis silviterrae	53.7	[51 - 56.4%]	30.48

References

1. Hanson RS, Hanson TE. Methanotrophic bacteria. Microbiol Rev. 1996 Jun;60(2):439–71.

2. Milich L. The role of methane in global warming: where might mitigation strategies be focused? Glob Environ Change. 1999 Oct 1;9(3):179–201.

3. Oremland RS, Culbertson CW. Importance of methane-oxidizing bacteria in the methane budget as revealed by the use of a specific inhibitor. Nature. 1992 Apr;356(6368):421–3.

4. Henneberger R, Lüke C, Mosberger L, Schroth MH. Structure and function of methanotrophic communities in a landfill-cover soil. FEMS Microbiol Ecol. 2012 Jul 1;81(1):52–65.

5. Knief C. Diversity and Habitat Preferences of Cultivated and Uncultivated Aerobic Methanotrophic Bacteria Evaluated Based on pmoA as Molecular Marker. Front Microbiol. 2015;6:1346.

6. Bowman JP, Sly LI, Nichols PD, Hayward AC. Revised taxonomy of the methanotrophs: description of Methylobacter gen. nov., emendation of Methylococcus, validation of Methylosinus and Methylocystis species, and a proposal that the family Methylococcaceae includes only the group I methanotrophs. Int J Syst Evol Microbiol. 1993 Oct 1;43(4):735–53.

7. Wartiainen I, Hestnes AG, McDonald IR, Svenning MM. Methylocystis rosea sp. nov., a novel methanotrophic bacterium from Arctic wetland soil, Svalbard, Norway (78° N). Int J Syst Evol Microbiol. 2006;56(3):541–7.

8. Lindner AS, Pacheco A, Aldrich HC, Costello Staniec A, Uz I, Hodson DJ. Methylocystis hirsuta sp. nov., a novel methanotroph isolated from a groundwater aquifer. Int J Syst Evol Microbiol. 2007 Aug 1;57(8):1891–900.

9. Dedysh SN, Belova SE, Bodelier PLE, Smirnova KV, Khmelenina VN, Chidthaisong A, et al. Methylocystis heyeri sp. nov., a novel type II methanotrophic bacterium possessing “signature” fatty acids of type I methanotrophs. Int J Syst Evol Microbiol. 2007 Mar;57(Pt 3):472–9.

10. Belova SE, Kulichevskaya IS, Bodelier PLE, Dedysh SN. Methylocystis bryophila sp. nov., a facultatively methanotrophic bacterium from acidic Sphagnum peat, and emended description of the genus Methylocystis (ex Whittenbury et al. 1970) Bowman et al. 1993. Int J Syst Evol Microbiol. 2013 Mar 1;63(3):1096–104.

11. Tikhonova EN, Grouzdev DS, Avtukh AN, Kravchenko IK. Methylocystis silviterrae sp.nov., a high-affinity methanotrophic bacterium isolated from the boreal forest soil. Int J Syst Evol Microbiol. 2021 Dec 16;71(12).

12. Kaise H, Sawadogo JB, Alam MS, Ueno C, Dianou D, Shinjo R, et al. Methylocystis iwaonis sp. nov., a type II methane-oxidizing bacterium from surface soil of a rice paddy field in Japan, and emended description of the genus Methylocystis (ex Whittenbury et al. 1970) Bowman et al. 1993. Int J Syst Evol Microbiol. 2023;73(6):005925.

13. Chen S, Zhou Y, Chen Y, Gu J. fastp: an ultra-fast all-in-one FASTQ preprocessor. Bioinformatics. 2018 Sep 1;34(17):i884–90.

14. Souvorov A, Agarwala R, Lipman DJ. SKESA: strategic k-mer extension for scrupulous assemblies. Genome Biol. 2018 Oct 4;19(1):153.

15. Parks DH, Imelfort M, Skennerton CT, Hugenholtz P, Tyson GW. CheckM: assessing the quality of microbial genomes recovered from isolates, single cells, and metagenomes. Genome Res. 2015 Jul;25(7):1043–55.

16. O'Leary NA, Wright MW, Brister JR, Ciufo S, Haddad D, McVeigh R, et al. Reference sequence (RefSeq) database at NCBI: current status, taxonomic expansion, and functional annotation. Nucleic Acids Res. 2016 Jan 4;44(D1):D733-745.

17. Sayers EW, Beck J, Brister JR, Bolton EE, Canese K, Comeau DC, et al. Database resources of the National Center for Biotechnology Information. Nucleic Acids Res. 2020 Jan 8;48(D1):D9–16.

18. Chan PP, Lin BY, Mak AJ, Lowe TM. tRNAscan-SE 2.0: improved detection and functional classification of transfer RNA genes. Nucleic Acids Res. 2021 Sep 20;49(16):9077–96.

19. Kanehisa M. Toward understanding the origin and evolution of cellular organisms. Protein Sci. 2019 Nov;28(11):1947–51.

20. Camacho C, Coulouris G, Avagyan V, Ma N, Papadopoulos J, Bealer K, et al. BLAST+: architecture and applications. BMC Bioinformatics. 2009 Dec 15;10:421.

21. Aramaki T, Blanc-Mathieu R, Endo H, Ohkubo K, Kanehisa M, Goto S, et al. KofamKOALA: KEGG Ortholog assignment based on profile HMM and adaptive score threshold. Bioinformatics. 2020 Apr 1;36(7):2251–2.

22. Rodriguez-R LM, Konstantinidis KT. The enveomics collection: a toolbox for specialized analyses of microbial genomes and metagenomes. PeerJ Preprints. 2016 Mar 27;4(e1900v1).

23. Jain C, Rodriguez-R LM, Phillippy AM, Konstantinidis KT, Aluru S. High throughput ANI analysis of 90K prokaryotic genomes reveals clear species boundaries. Nat Commun. 2018 Nov 30;9(1):5114.

24. Na SI, Kim YO, Yoon SH, Ha SM, Baek I, Chun J. UBCG: Up-to-date bacterial core gene set and pipeline for phylogenomic tree reconstruction. J Microbiol. 2018 Apr;56(4):280–5.

25. Edgar RC. MUSCLE: a multiple sequence alignment method with reduced time and space complexity. BMC Bioinformatics. 2004 Aug 19;5(1):113.

26. Stamatakis A. RAxML version 8: a tool for phylogenetic analysis and post-analysis of large phylogenies. Bioinformatics. 2014 Jan 21;30(9):1312–3.

27. Lane DJ. 16S/23S rRNA sequencing. In: Nucleic acid techniques in bacterial systematics. John Wiley and Sons, New York; 1991. p. 115–75.

28. Goris J, Konstantinidis KT, Klappenbach JA, Coenye T, Vandamme P, Tiedje JMY 2007. DNA–DNA hybridization values and their relationship to whole-genome sequence similarities. Int J Syst Evol Microbiol. 57(1):81–91.

29. Konstantinidis KT, Tiedje JM. Genomic insights that advance the species definition for prokaryotes. PNAS. 2005 Feb 15;102(7):2567–72.

30. Konstantinidis KT, Tiedje JM. Towards a genome-based taxonomy for prokaryotes. J Bacteriol. 2005 Sep 15;187(18):6258–64.

31. Li C, Hambright KD, Bowen HG, Trammell MA, Grossart HP, Burford MA, et al. Global co-occurrence of methanogenic archaea and methanotrophic bacteria in Microcystis aggregates. Environ Microbiol. 2021 Nov;23(11):6503–19.

32. Seemann T. Prokka: rapid prokaryotic genome annotation. Bioinformatics. 2014 Jul 15;30(14):2068–9.

33. Price MN, Dehal PS, Arkin AP. FastTree 2 – Approximately Maximum-Likelihood Trees for Large Alignments. PLOS ONE. 2010 Mar 10;5(3):e9490.

34. Fotedar R, Sankaranarayanan K, Caldwell ME, Zeyara A, Al Malki A, Kaul R, et al. Reclassification of Facklamia ignava, Facklamia sourekii and Facklamia tabacinasalis as Falseniella ignava gen. nov., comb. nov., Hutsoniella sourekii gen. nov., comb. nov., and Ruoffia tabacinasalis gen. nov., comb. nov., and description of Ruoffia halotolerans sp. nov., isolated from hypersaline Inland Sea of Qatar. Antonie van Leeuwenhoek. 2021 Aug 1;114(8):1181–93.

35. Fotedar R, Caldwell ME, Sankaranarayanan K, Al -Zeyara A, Al-Malki A, Kaul R, et al. Ningiella ruwaisensis gen. nov., sp. nov., a member of the family Alteromonadaceae isolated from marine water of the Arabian Gulf. Int J Syst Evol Microbiol. 2020 Jul;70(7):4130–8.

36. Eren AM, Kiefl E, Shaiber A, Veseli I, Miller SE, Schechter MS, et al. Community-led, integrated, reproducible multi-omics with anvi'o. Nat Microbiol. 2021 Jan;6(1):3–6.

37. Hyatt D, Chen GL, LoCascio PF, Land ML, Larimer FW, Hauser LJ. Prodigal: prokaryotic gene recognition and translation initiation site identification. BMC Bioinformatics. 2010 Mar 8;11(1):119.

38. van Dongen S, Abreu-Goodger C. Using MCL to extract clusters from networks. Methods Mol Biol. 2012;804:281–95.

39. Galperin MY, Makarova KS, Wolf YI, Koonin EV. Expanded microbial genome coverage and improved protein family annotation in the COG database. Nucleic Acids Res. 2015 Jan;43(Database issue):D261-269.

40. Hobbie JE, Daley RJ, Jasper S. Use of nuclepore filters for counting bacteria by fluorescence microscopy. Appl Environ Microbiol. 1977 May;33(5):1225–8.

Chapter 2

Effect of Oxygen Concentration on the Methane-oxidizing Bacteria, *Methylosinus trichosporium* OB3b and *Methylomonas* sp. WSC-7

Abstract

Methane-oxidizing bacteria (MOB) play a crucial role in the global methane cycle, serving as significant actors in biogeochemical cycling. However, their physiological response to changing oxygen concentrations remains incompletely understood. This study investigates how two MOB species, *Methylosinus trichosporium* OB3b and *Methylomonas* sp. WSC-7, respond to changing oxygen concentrations and the addition of catalase, a hydrogen peroxide scavenger, in growth media. Transcriptomics analysis demonstrates that under high oxygen conditions, *M. trichosporium* OB3b upregulates genes involved in reactive oxygen species (ROS) defense, including cytochrome c peroxidase and superoxide dismutase, suggesting a need to deal with elevated ROS levels. Conversely, *Methylomonas* sp. WSC-7 exhibits cell clustering behavior, potentially as a defense mechanism against ROS toxicity. Differential expression of flagellar biosynthesis genes and chemotaxis response genes further supports this adaptive response. Moreover, *Methylomonas* sp. WSC-7 shows reduced expression of soluble methane monooxygenase genes under low oxygen conditions, while *M. trichosporium* OB3b exhibits higher expression under catalase-amended conditions, and that rates of methane oxidation for both strains are impacted by the concentration of oxygen and amending the growth media with catalase. Our findings underscore the importance of oxygen concentration in modulating MOB physiology and suggest potential strategies for optimizing their growth conditions.

Introduction

Methane-oxidizing bacteria (MOB) are organisms that can oxidize methane as their primary carbon and energy source. These bacteria oxidize methane to CO_2 using a pathway involving conversion of methane to methanol, and further to formaldehyde and formate where the carbon is assimilated by the ribulose monophosphate pathway or the serine pathways (1). Methane is a potent greenhouse gas (2), and these organisms play a significant role in the global methane cycle (3). Studying this group of organisms is critical for understanding their total impact on biogeochemical cycling. Also, isolating and characterizing novel species of methane oxidizers will be useful in biotechnological applications such as bioremediation and generation of value-added products (4). All of these areas of study require detailed understanding of MOB physiology and conditions for optimized growth.

During aerobic metabolism toxic reactive oxygen species (ROS) are generated including superoxide and hydrogen peroxide (5–9). Because endogenous ROS generation in bacteria is a result of cellular respiration, increases in endogenous production in ROS generated during bacterial respiration is positively correlated with increases in cellular metabolic rate as well as elevated O_2 concentrations (5–7,10–12). This endogenous production of ROS can have harmful effects on cells including damaging proteins, nucleic acids, and lipids (10). In addition to the potential generation of toxic ROS by cellular respiration, aerobic MOB oxidize methane using a class of enzymes called methane monooxygenases. These enzymes catalyze the oxidation of methane to methanol in the presence of dioxygen, and this reaction may contribute to ROS generation (13). Some studies have demonstrated that the enzyme activity of methane

monooxygenases may catalyze the production of hydrogen peroxide, and that monooxygenases are inhibited by the presence of hydrogen peroxide leading to decreased enzyme activity (8,14).

Many species of bacteria, including MOB, have evolved systems to counteract the negative effects of ROS. The primary defense systems employed use ROS scavenging enzymes such as catalase, cytochrome c peroxidases, and superoxide dismutase to decrease ROS concentrations (10,15). The general bacterial response to increases in H_2O_2 accumulation includes the expression of a wide set of peroxidase class enzymes that reduce H_2O_2 to H_2O governed by the OxyR regulon (16). H_2O_2 can also be reduced by cytochrome c peroxidase, and it has even been shown in MOB that cytochrome c peroxidase may serve to remediate peroxide buildup from cellular respiration (15). In bacteria, superoxide is scavenged primarily by the enzyme superoxide dismutase that catalyzes the dismutation of superoxide into H_2O_2 and O_2, governed by the SoxRS regulatory system (16).

In addition to using ROS scavenging enzymes to mitigate ROS buildup, some species of bacteria that are known to be sensitive to elevated oxygen levels even employ the use of cell clustering to defend against oxygen stress (17). Some microaerophilic bacteria have chemotaxis sensors that regulate the motility of cells in the presence of unfavorable oxygen concentrations leading to cell clumping which may protect the cells from elevated oxygen by reducing the surface-to-volume ratio of the cells by limiting oxygen diffusion (17-19). However, despite our understanding of ROS defense systems such as these, the precise way that MOB deal with the consequences of ROS, or even how they respond to changes in oxygen concentration is not well understood.

An experiment using transcriptomics analysis was designed to show how two species of MOB, *Methylosinus trichosporium* OB3b and *Methylomonas* sp. WSC-7, respond to changing oxygen concentrations and how the use of growth media amended with catalase as a hydrogen peroxide

scavenger influences the growth and physiology of the two strains. This experiment demonstrated that amending growth media with catalase leads to an increase in methane oxidation rate for both *M. trichosporium* OB3b and *Methylomonas* sp. WSC-7. Also, *M. trichosporium* OB3b responds to increases in oxygen concentration by overexpressing cytochrome c peroxidase and superoxide dismutase encoding genes, but *Methylomonas* sp. WSC-7 responds to increases in oxygen concentration by cell clustering and decreasing expression of flagella biosynthesis genes and aerotaxis response genes.

Methods

Growth Conditions of *M. trichosporium* OB3b and *Methylomonas* sp. WSC-7

The objective of this study was to determine if changes in headspace oxygen concentration and/or the addition of catalase to the growth media influenced the physiology, response to ROS toxicity, and methane oxidation rate of two strains of methane-oxidizing bacteria, *M. trichosporium* OB3b and *Methylomonas* sp. WSC-7 grown under methane-oxidizing conditions.

M. trichosporium OB3b cells were grown statically in modified nitrate mineral salts medium (NMS) similar to the medium developed by Whitenbury et al. (20) for the growth of methane-oxidizing bacteria in the group's initial characterization studies, but with the addition of a vitamin solution. The modified NMS medium contains (per liter of distilled water) 1 g KNO_3, 0.27 g KH_2PO_4, 1 g $MgSO_4 \cdot 7H_2O$, 0.14 g $CaCl_2 \cdot 2H_2O$, and 0.23 g Na_2HPO_4, 0.5% (v/v) acidic trace element solution (AcTES), 0.02% alkaline trace element solution (AlTES), and 1% vitamin solution. AcTES contains (per liter), 2 g $FeSO_4 \cdot 7H_2O$, 0.07 g $ZnSO_4 \cdot 7H_2O$, 0.5 g $MnCl_2 \cdot 4H_2O$, 0.12 g $CoCl_2 \cdot 6H_2O$, 0.01 g $NiCl_2 \cdot 6H2O$, 0.5 g $CuSO_4$, 0.01 g H_3BO_3, 0.06 g

$LaNO_3$, 0.06 g $CeNO_3$, and 100 mM HCl. The AlTES contains (per liter) 0.11 g Na_2SeO_4, 0.05 g Na_2WO_4, 0.29 g Na_2MoO_4, and 0.04 g NaOH. The vitamin solution contains (per liter) 5 mg 4-aminobenzoic acid, 2 mg D-biotin, 2 mg folic acid, 10 mg pyridoxine-HCl, 5 mg riboflavin, 5 mg thiamine-HCl x $2H_2O$, 5 mg nicotinic acid, 5 mg calcium D-pantothenate, 5 mg thioctic acid (α-Lipoic Acid), and 0.10 mg vitamin B12.

Methylomonas sp. WSC-7 cells were grown statically in HEPES/phosphate buffered Saddle Mountain Creek medium (HPB-SMC Medium). This contains (per liter of distilled water) 2.38 g HEPES (Free Acid), 0.26 g NaCl, 0. 14 g Na_2HPO_4, 0.11 g KCl, 0.12 $MgSO_4 \cdot 7H_2O$, 0.04 g $NaNO_3$, 0,04 g $CaCl_2 \cdot 2H_2O$, 0.004 g H_3BO_3, and 0.007 g $SrCl_2 \cdot 6H_2O$ as well as 0.5% (v/v) AcTES, 0.02% alkaline trace element solution AlTES, and 1% vitamin solution.

Three treatments were evaluated in this study. The strains were grown statically in 500 mL of respective media in 1 L stoppered bottles, leaving 500 mL of available gas headspace. One condition (high oxygen) was grown with a headspace gas composition of 69% N_2, 10% CH_4, and 21% O_2. The second condition (low oxygen) was grown with a headspace gas composition of 85% N_2, 10% CH_4, and 5% O_2. The third condition (catalase) was grown at high oxygen, but the medium was amended with 20 µg/mL of catalase (From Bovine Liver, Thermo Scientific). Each condition was incubated at 28 °C without shaking and methane depletion was measured by gas chromatography on a Shimadzu GC-14A gas chromatograph (Shimadzu, Japan). Methane oxidation rates (MOR) were calculated as $MOR=\ln(\Delta[CH_4])/\ln(\Delta t)$. This is the slope of the natural log of the methane depletion curve where $[CH_4]$ is the molar concentration of CH_4 and t is time elapsed in hours.

RNA Extraction, Illumina Sequencing Library Preparation, and Sequencing

Cells for RNA extraction were grown staticallly in one-liter bottles with 500 ml of medium and harvested in late log phase by centrifugation for 20 minutes at 4 °C and 4000 x g using an Eppendorf 5910 centrifuge with cell pellets stored at -80 °C. The Zymo Research Quick-RNA Fungal/Bacterial Miniprep kit was used for RNA extraction. Additional DNase treatments were carried out using the Invitrogen DNase I Amplification Grade treatment kit. Nucleic acid extracts were quantified using a Qubit Fluorometer 2.0 with RNA high specificity and DNA broad range specificity reagent kits.

Illumina compatible sequencing libraries were prepared for sequencing with the Zymo-Seq RiboFree Total RNA Library Kit (Zymo Research, USA) according to the manufacturer's specifications. Prior to sequencing, the cDNA library was concentrated using a Thermo Scientific Savant DNA120 SpeedVac Concentrator, and size selection was carried out using the Agilent 4150 TapeStation System.

Sequencing of the final cDNA library was performed at the Oklahoma Medical Research Foundation Center for Clinical Genomics (Oklahoma City, USA) using Illumina NovaSeq 6000 S4 PE150 chemistry.

Reference Genome Sequencing

Genomic DNA of *Methylomonas.* sp. WSC-7 from a log-phase grown culture grown in the modified NMS medium at 28 °C was extracted using the Qiagen DNeasy Blood and Tissue Kit. DNA was fragmented using a QSonica 800R3 sonicator and built into Illumina-compatible shotgun libraries using the KAPA HyperPrep Kit. Shotgun libraries were sequenced on an Illumina MiSeq instrument. Sequence data was processed using fastp v0.23.2 (21) to remove

reads containing uncalled bases ('N'), trim low-quality bases (q < 30), and merge overlapping reads. The resulting analysis-ready reads were used as input for de novo assembly with SKESA v2.5.1 (22). The quality of genomes was assessed by CheckM v1.1.3 (23). The genome for *M. trichosporium* OB3b (GCF_000178815.2) was downloaded from the NCBI RefSeq database (24). Gene prediction was performed using Prodigal v2.6.3 (25) and barrnap v0.9 (26).

Read Mapping and Quantification

Raw fastq reads were filtered for high quality reads (q < 30) and the adaptors were trimmed using fastp v0.22.0 (21). Quality filtered pair-end reads were mapped to respective reference genomes using Bowtie 2 v2.2.5 (27). The .bam files generated were parsed for DNA contamination issues by removing reads known to directionally be linked to genomic DNA, then removing an equal number of reads from the RNA pool to account for bias. The precomputed alignments generated by Bowtie 2 were used as input for transcript quantification using Salmon 0.14.2 (28).

Differential Expression Analysis

The R program DESeq2 was used for differential expression analysis of quantified reads using the likelihood ratio test method (29). Genes that were differentially expressed (adjusted p-value < 0.05, log2FC < -2 or > 2) were annotated using KEGG BlastKOALA (30).

Scanning Electron Microscopy of Biofilms

Methylomonas sp. WSC-7 cells for scanning electron microscopy were grown statically to late-log phase in HPB-SMC media with 10% CH_4 added to the headspace of air. Cells were filtered onto a 0.2 mm membrane (Whatman) by vacuum filtration and the filtered cells are transferred onto a poly-l-lysine coated slide.

The cells were then fixed in HPB-SMC medium with 4% glutaraldehyde for 17 hours at room temperature and then washed for 10 minutes, three times in HPB-SMC medium to remove excess fixative. After fixation, cells were immersed in a 1% OsO_4 solution in modified NMS medium at 4 °C for 1 hour and washed again with deionized water to remove the excess solution. Cells were then dehydrated by immersion for 10 minutes each in 25%, 50%, 70%, 85%, 95%, and three times in 100% ethanol (in deionized water). Critical point drying occurred using a Tousimis Autosamdri-814 and samples were sputter coated with a thin layer (~ 4 nm) of iridium (Ir) using an EMS Quorum Q150 ES Plus sputter coater. Imaging of the biofilms was performed at the University of Oklahoma Samuel Roberts Noble Microscopy Laboratory using a Zeiss Neon 40 EsB field emission scanning electron microscope at 5 kV.

Results

Effect of Catalase and Oxygen Concentration on *M. trichosporium* OB3b and *Methylomonas* sp. WSC-7 Methane Oxidation Rate

The methane oxidation rate (MOR) was measured for both *M. trichosporium* OB3b and *Methylomonas* sp. WSC-7 across the three treatments. Both *M. trichosporium* OB3b and *Methylomonas* sp. WSC-7 had a significantly higher MOR under the catalase amended conditions compared to both the high oxygen condition and the low oxygen condition. Also, MOR was higher in the high oxygen condition with no catalase compared to the low oxygen condition for both strains. (**Fig. 1**).

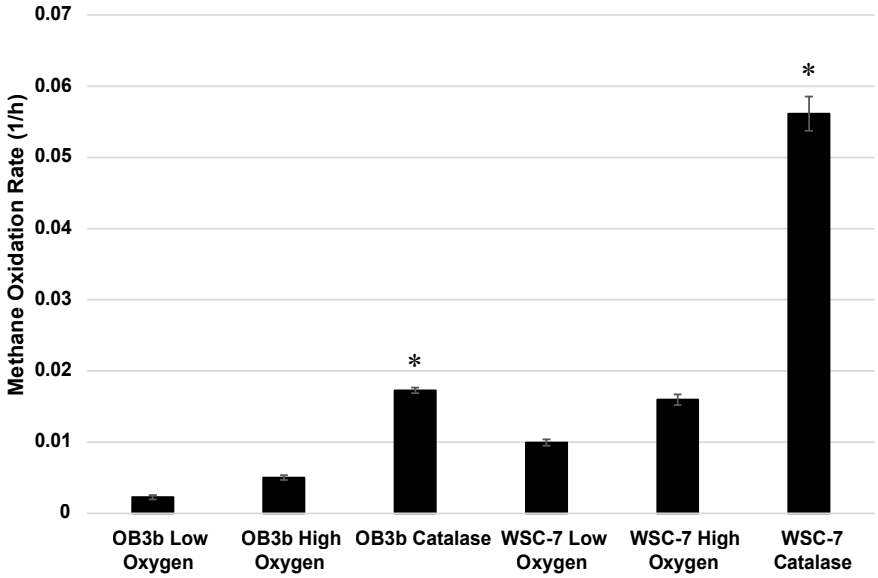

Figure 1: Methane oxidation rates of two methane oxidizing bacterial strains *Methylosinus trichosporium* OB3b and *Methylomonas* sp. WSC-7 grown in low (5%) headspace oxygen, high (21%) headspace oxygen, or in high oxygen with catalase amending the growth media. Each condition was incubated with a headspace methane concentration of 10%. Data are shown as the mean +/- standard deviation across triplicate samples. Significantly elevated methane oxidation rates (p-value < 0.05) are noted by *.

RNA-seq of *M. trichosporium* OB3b and *Methylomonas* sp. WSC-7

To explain these trends in the MORs and the overall physiological response to oxygen concentration and catalase on the two strains, gene expression profiles were analyzed by DESeq2. The likelihood ratio test (LRT) of our differential gene expression analysis demonstrated that 136 genes were significantly differentially expressed (log2 Fold Change > 2.0 or < -2.0 & adjusted p-value < 0.05) by *M. trichosporium* OB3b across all conditions and that 998 genes were differentially expressed by *Methylomonas* sp. WSC-7. The differentially expressed genes were annotated by KEGG's BlastKOALA. A total of 55 differentially expressed genes from *M. trichosporium* OB3b and 599 genes from *Methylomonas* sp. WSC-7 were annotated.

M. trichosporium OB3b & *Methylomonas* sp. WSC-7 ROS Gene Expression

There were notable differences in the ROS gene expression profiles across different conditions. *M. trichosporium* OB3b overexpressed a cytochrome c peroxidase gene when grown at high oxygen. Expression of this gene decreased when grown with catalase and decreased even more when grown at low oxygen (**Fig. 2**). The same trend can be observed for the *katG* gene encoding for catalase-peroxidase in OB3b. However, the change in expression is not statistically significant (adjusted p-value = 0.14). Additionally, in OB3b a gene encoding for superoxide dismutase was underexpressed in the catalase condition compared to both the high oxygen and low oxygen conditions. This same gene was expressed the greatest in the low oxygen condition (**Fig. 2**). The decreased expression of these genes when catalase is added to the growth medium further implies that these genes are involved in ROS remediation and that the addition of catalase may aid in ROS remediation during growth on methane, reducing the need for OB3b to produce ROS defense enzymes.

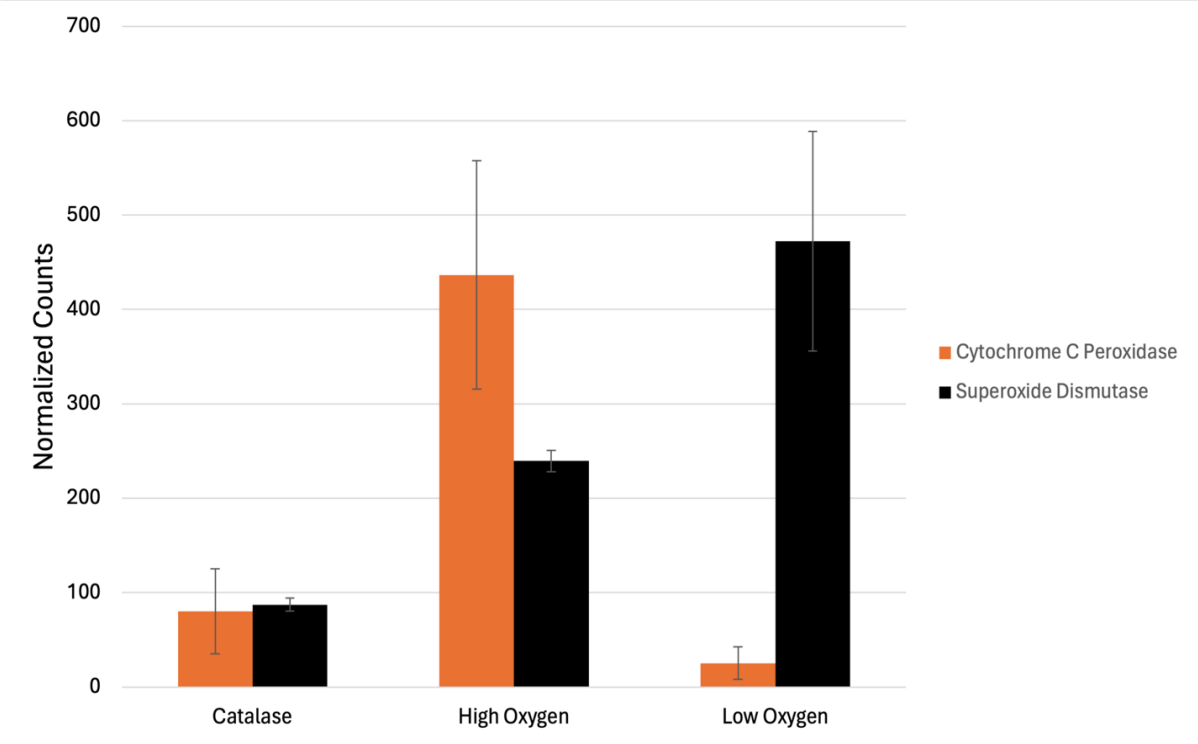

Figure 2: Normalized counts of Cytochrome c Peroxidase and Superoxide Dismutase genes in *M. trichosporium* OB3b across high oxygen, low oxygen, and catalase containing conditions. Data are shown as the +/- standard deviation of triplicate samples.

Methylomonas. sp. WSC-7 also expresses a cytochrome c peroxidase that could be reducing H_2O_2. However, unlike in *M. trichosporium* OB3b, the highest expression level is in the low oxygen condition with less in the catalase condition, and in the high oxygen condition it is expressed at very low levels if at all (**Fig. 3**). There is also a superoxide dismutase gene being differentially expressed in sp. WSC-7. This gene is expressed at low oxygen, far less at high oxygen condition, and not at all in the catalase condition (**Fig. 3**). This trend leads us to hypothesize that under elevated oxygen conditions, *Methylomonas* sp. WSC-7 uses a method of ROS defense that is distinct from OB3b. Based on observations of cell clustering under growth

conditions of high oxygen and that this cell cluster is lacking when oxygen is lower (**Fig. 4**), strain WSC-7 may cluster together to reduce the diffusion of oxygen to the cells as a primary means of dealing with increased aeration. In addition to the observed cell clustering, *Methylomonas* sp. WSC-7 expressed several genes associated with flagellar biosynthesis proteins and flagellar component proteins (*flgBCDEFGHIK*) to a much greater extent in the low oxygen conditions than in high oxygen or catalase amended conditions (**Fig. 5**). Additionally, the *cheBDRV* chemotaxis protein genes are expressed at higher levels in the low oxygen condition as well (**Fig. 5**). The increase in the expression of flagellar protein synthesis genes and chemotaxis response genes suggests that there is increased motility in the low oxygen condition, perhaps as an aerotaxis response to facilitate access to oxygen when the concentration is lower.

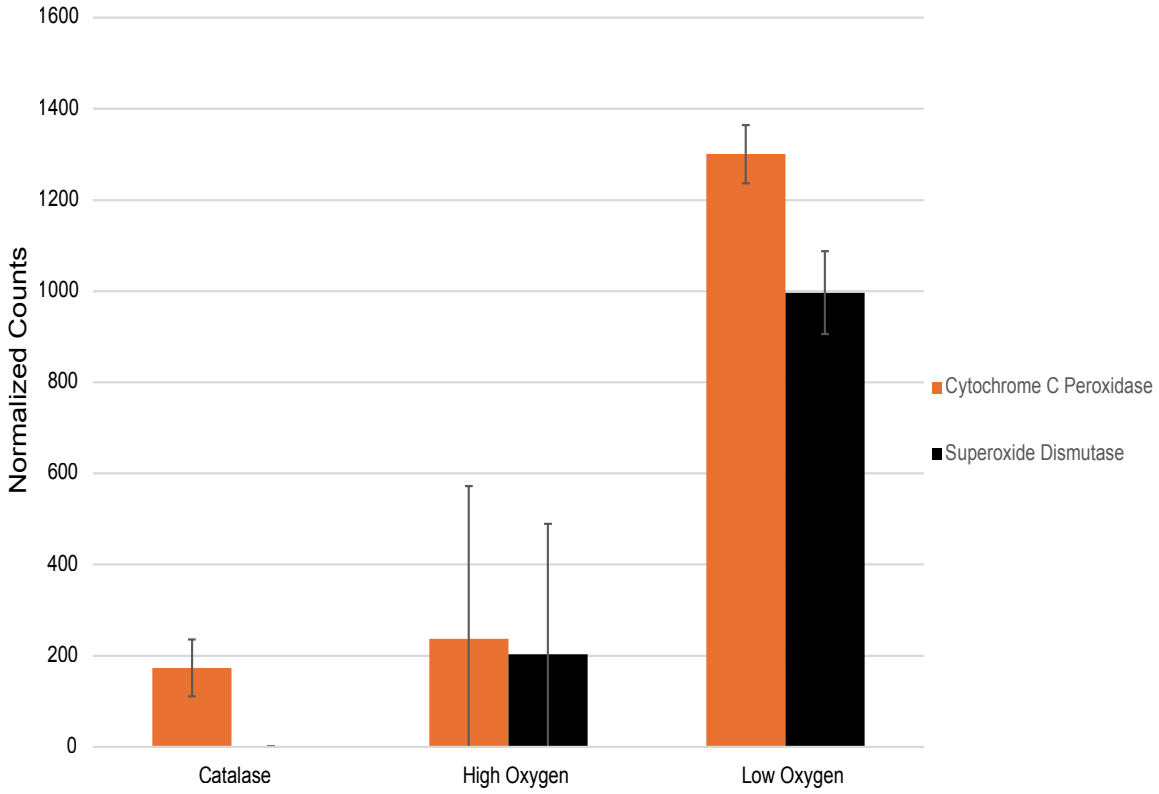

Figure 3: Normalized gene counts of Cytochome C Peroxidase and Superoxide Dismutase genes in *Methylomonas* sp. WSC-7 across high oxygen, low oxygen, and catalase containing conditions. Each condition was incubated with a headspace methane concentration of 10%. Data are shown as the mean +/- standard deviation across triplicate samples for the High Oxygen and Low Oxygen conditions and duplicate samples for the Catalase condition.

Figure 4: Representative samples of Methylomonas sp. WSC-7 growing in high oxygen, low oxygen, and catalase conditions depicting that in conditions where the headspace oxygen is 21% the cells form clumps and when the headspace oxygen is at 5% the culture is turbid and there is no visible clumping.

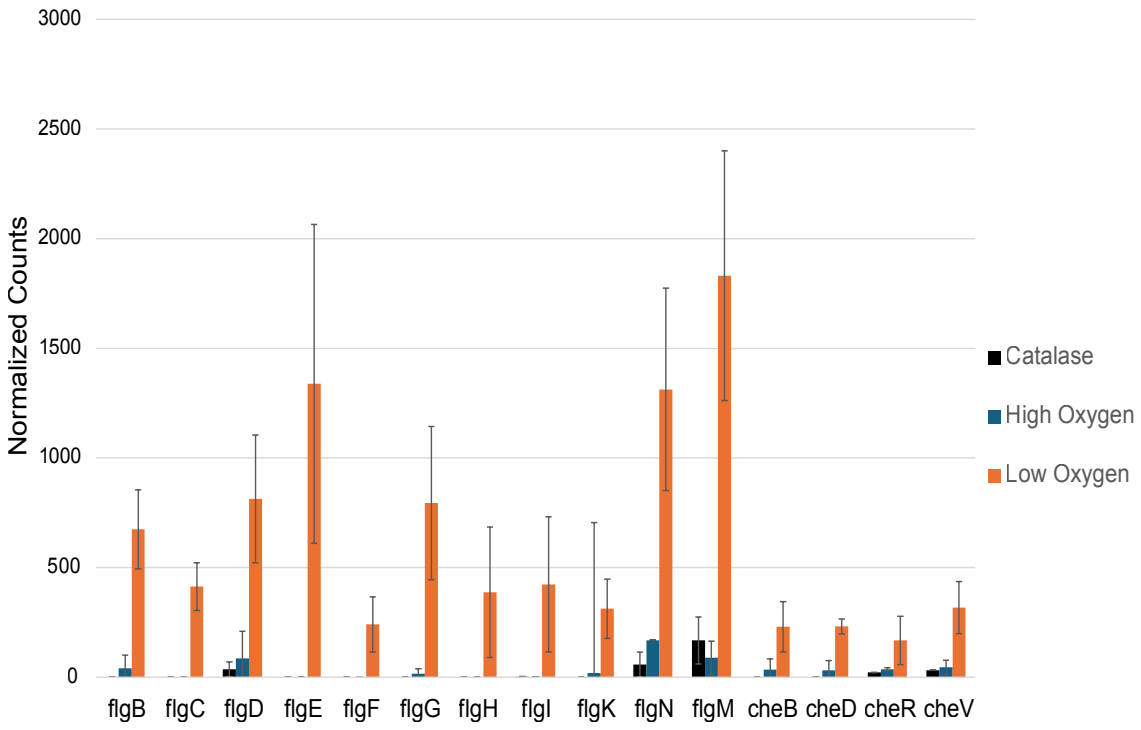

Figure 5: Normalized gene counts of flagella biosynthesis genes and chemotaxis reponse genes in Methylomonas sp. WSC-7 across high oxygen, low oxygen, and catalase containing conditions. Each condition was incubated with a headspace methane concentration of 10%. Data are shown as the mean +/- standard deviation across triplicate samples for the high oxygen and low oxygen conditions and duplicate samples for the catalase condition.

M. trichosporium OB3b & *Methylomonas* sp. WSC-7 Methane Oxidation Pathway Gene Expression

The WSC-7 *pmoABC* genes coding for the particulate methane monooxygenase are expressed at much greater levels than the *mmoXYC* genes in all conditions (**Fig. 6**). For the *pmoABC* genes there is not a statistically significant change in expression under any condition. However, the expression of each of the *mmoXYC* genes is significantly lower in the low oxygen condition. In WSC-7, the methanol dehydrogenase genes *xoxF* and *mxaF* are expressed in all conditions with *xoxF* showing increased expression under low oxygen. In OB3b, there are no statistically

significant changes in MMO protein gene expression levels (**Fig. 7**). Further, in OB3b, the *mxaF* and *xoxF* methanol dehydrogenases are expressed at similar levels in each condition (**Fig. 7**).

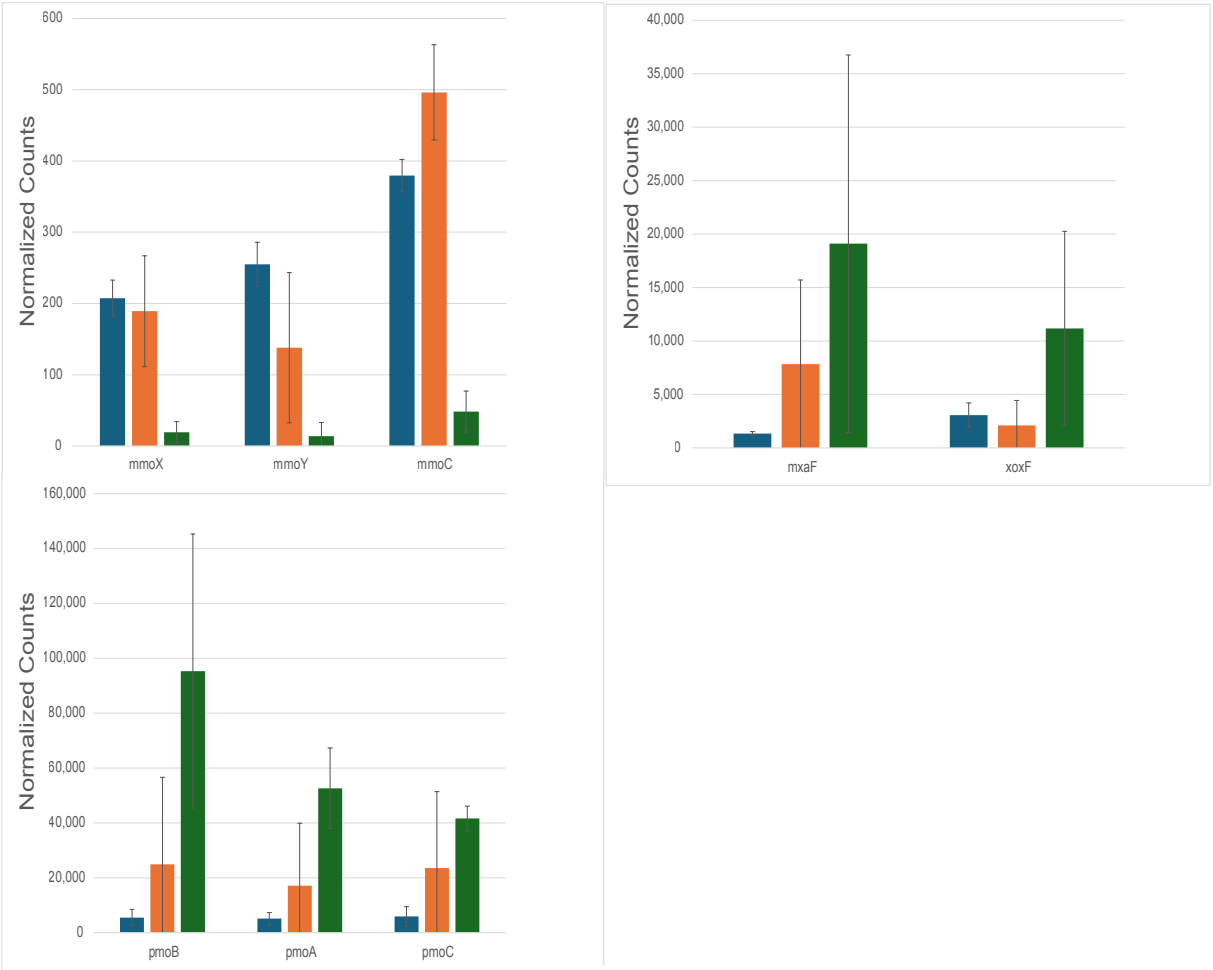

Figure 6: Normalized counts of methane and methanol oxidation genes by *Methylomonas* sp. WSC-7 in catalase (blue), high oxygen (orange), and low oxygen (green), conditions. Data are shown as the +/- standard deviation across triplicate samples for the high and low conditions and duplicate samples for the catalase condition.

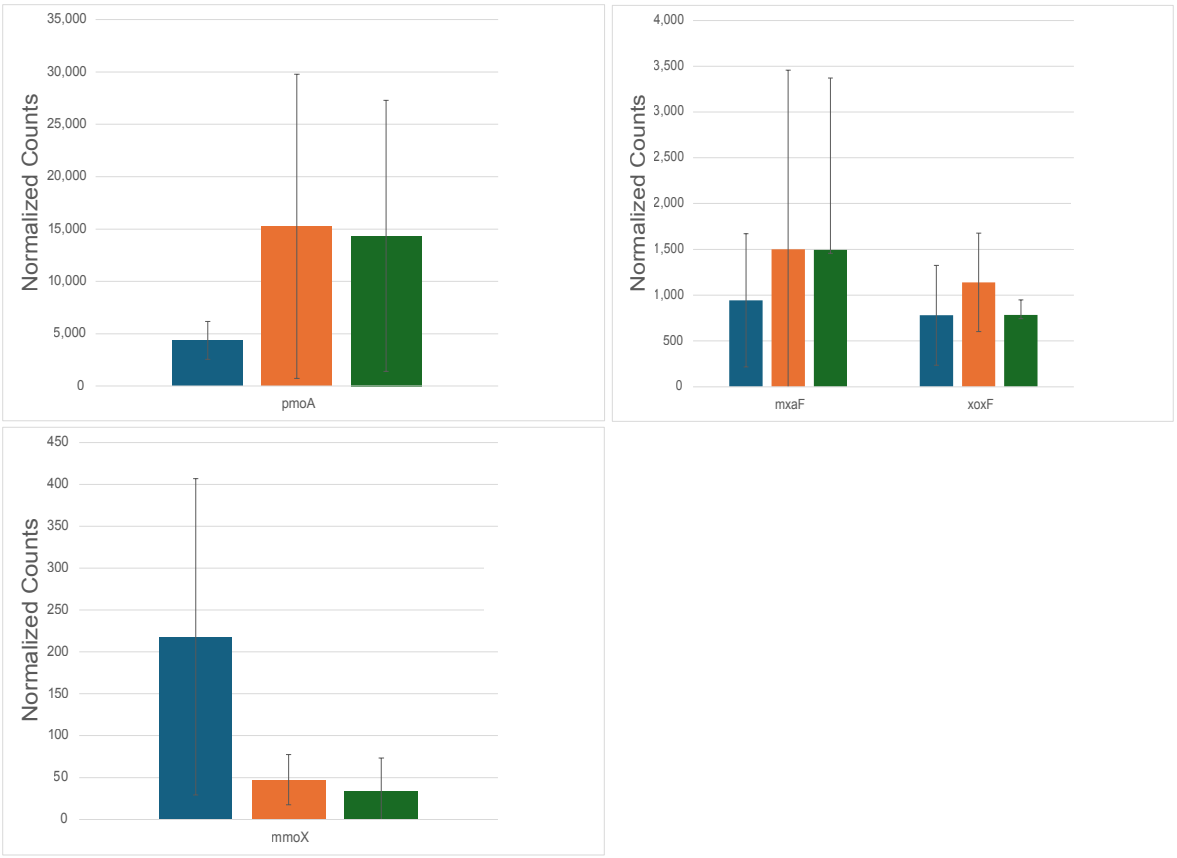

Figure 7: Normalized counts of methane and methanol oxidation genes by *M. trichosporium* OB3b in catalase (blue), high oxygen (orange), and low oxygen (green) conditions. Data are shown as the +/- standard deviation across triplicate samples for the high and low conditions and duplicate samples for the catalase condition.

Methylomonas sp. WSC-7 Growth Phenotypes in Changing Oxygen Concentrations and Scanning Electron Microscopy of WSC-7 Biofilms

The cells of *Methylomonas* sp. WSC-7 were observed to form clumps which floated in the high oxygen conditions, but not at low oxygen (**Fig. 4**). However, biofilms were observed using electron microscopy under all conditions. Although the cells did not appear to form a biofilm in the bottles when growing in the low oxygen conditions, they appear to have the same cell stacking structure as the cells growing in the high oxygen and catalase conditions when observing the scanning electron micrographs (**Fig. 8**). This suggests the capacity form clumps was present under all conditions, but only visible at high oxygen.

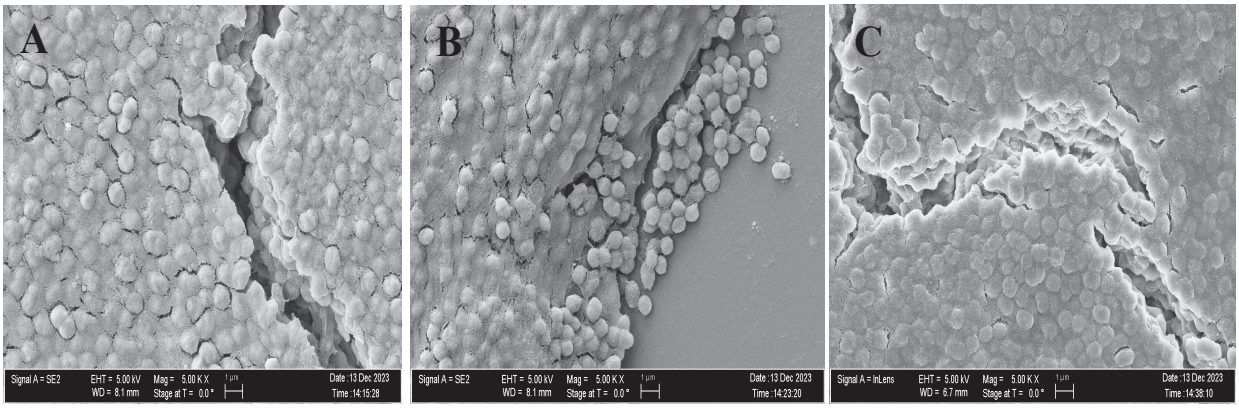

Figure 8: Representative scanning electron micrographs of *Methylomonas* sp. WSC-7 cells grown in catalase (A) high oxgyen (B) and low oxygen (C) conditions. Images were captured at 5000X zoom and electron high tension of 5 kV.

Discussion

Lower Oxygen Concentrations Leads to Lower Expression of Soluble Methane Monooxygenase in *Methylomonas* sp. WSC-7

It has been determined that genes encoding the soluble methane monooxygenase in the type I MOB WSC-7 are more impacted by decreases in oxygen concentration than those of the genes for particulate methane monooxygenase. WSC-7 in low oxygen had decreased expression of *mmoXYC* genes. Interestingly, the same trend was not present in type II MOB OB3b. In OB3b, there was a slightly higher expression of *mmoX* under the catalase condition, but this change was not statistically significant and gene expression in high and low oxygen conditions was similar. Other studies have demonstrated that in wild-type OB3b and OB3b mutants that are unable to express genes for particulate methane monooxygenase, increases in oxygen concentration from 10% headspace O_2 to 80% headspace O_2 decreased sMMO protein levels and enzyme activity (31). This study did not see a change in expression of the sMMO gene *mmoX* for Ob3b, but ranges of O_2 examined in this study were from 5% to 21% which may account for this discrepancy. Perhaps this observation suggests that oxygen levels impact type I and type II MOB sMMO genes differently.

Methylosinus trichosporium OB3b May Remediate Negative Impacts on MOR by Expression of Cytochrome c Peroxidase and Superoxide Dismutase

Changing the headspace oxygen concentration and/or amending the growth medium with 20 µg/mL of catalase impacted the MOR and gene expression profile of methane-oxidizing bacteria when they are growing in pure culture. *M. trichosporium* OB3b had genes related to the remediation of radical oxygen toxicity including cytochrome c peroxidase and superoxide

dismutase (SOD) overexpressed in the high oxygen condition compared to when catalase was used to amend the media, or when there was a lower concentration of headspace O_2.

This observation that when O_2 concentration is higher, the expression of ROS defense genes in OB3b increases is plausible. It has been demonstrated that when aerobically growing cells are exposed to elevated oxygen concentrations, there is a proportional increase in the accumulation of ROS such as superoxide and hydrogen peroxide inside cells (10, 32-34). Specifically, the observation that cytochrome c peroxidase is one of the enzymes that is used by OB3b to mitigate hydrogen peroxide buildup is also supported by previous experiments. It has been demonstrated that cytochrome c peroxidase from *Methylococcus capsulatus* Bath is capable of peroxide reduction. Researchers in that study speculate that because of the peroxide formation induced by monooxygenase O_2 activation, peroxide toxicity remediation could be a reasonable role for the protein (15).

In *M. trichosporium* OB3b, the superoxide dismutase encoding gene is also differentially expressed in the same manner, where at a higher headspace oxygen concentration, the gene is expressed more. This could happen for potentially the same reason, as a means of scavenging toxic superoxide radicals which have been shown to be generated by bacterial aerobic metabolism and cause cellular damage (7,9,35).

Methylomonas sp. WSC-7 May Utilize Cell Clumping to Defend Against ROS Toxicity

These data suggest that WSC-7 cells are clustering together as a way to defend against ROS toxicity when exposed to unfavorably high concentrations of O_2. At higher O_2 concentrations the *Methylomonas* sp. WSC-7 cells tend to clump together to form flocs, but when growing in the low O_2 condition, the cells disperse throughout the growth medium (**Fig. 4**). This correlates with

increased expression of flagellar biosynthesis protein genes in the low oxygen condition. Since the flagellar protein genes are downregulated in the high oxygen condition, this could lead to less motility, and reduction in cell dispersal. Moreover, biofilm formation consists of a transition of motility to non-motility by bacterial cells to facilitate cell-to-cell adhesion (36) so it is plausible that when clustered, expression of flagellar proteins is shut down. The WSC-7 cell aggregation could serve as a defense against elevated oxygen exposure because there is a reduction in the surface-to-volume ratio of the cells by limiting oxygen diffusion (19). Further, it was observed that *Methylomonas* sp. WSC-7 was shown to have higher expression of the *cheB, cheD, cheR, and cheV* genes under conditions of low oxygen. It has been shown that *A. brasilense* mutants that have been unable to express *cheB* or *cheR* genes are shown have an impaired aerotaxis response even though the cells remain motile (37). This may suggest that the differentially expressed *che* genes are important to properly navigating to oxygen. Also, *A. brasilense* cells have been shown to cluster together under elevated oxygen concentrations and *A. brasilense* mutants lacking their ability to express chemotaxis genes clump together more frequently (17,18). This makes sense, as *A. brasilense* has been shown to avoid unfavorable oxygen concentrations that are either too high or too low via aerotaxis (38). Strain WSC-7 likely does the same, where under conditions that are oxygen-rich, the cells clump together, but under lower oxygen conditions, the cells are motile and migrate towards oxygen concentrations that optimize oxygen exposure to the cells. However, this may come with having to compensate for ROS toxicity by expressing peroxidase and SOD genes as observed here.

Some key conclusions arise from these findings. The type II methanotroph *M. trichosporium* OB3b transcribes genes needed to mitigate the toxic effects of ROS more when growing at elevated O_2 concentrations, but the type I methanotroph *Methylomonas* sp. WSC-7 appears to

mitigate the toxic effects of ROS differently than OB3b by facilitating cell clumping as a potential defense mechanism from ROS toxicity. While this study is limited to just two different strains of MOB, the fact that there such a drastic distinction in their behavior demonstrates that when trying to optimize growth conditions for the isolation, cultivation and biotechnical implication of MOB, the consideration of oxygen concentration is critical and has an impact on cellular metabolism and physiology.

References

1. Hanson RS, Hanson TE. Methanotrophic bacteria. Microbiol Rev. 1996 Jun;60(2):439–71.

2. Milich L. The role of methane in global warming: where might mitigation strategies be focused? Glob Environ Change. 1999 Oct 1;9(3):179–201.

3. Oremland RS, Culbertson CW. Importance of methane-oxidizing bacteria in the methane budget as revealed by the use of a specific inhibitor. Nat. 1992 Apr;356(6368):421–3.

4. Guerrero-Cruz S, Vaksmaa A, Horn MA, Niemann H, Pijuan M, Ho A. Methanotrophs: Discoveries, Environmental Relevance, and a Perspective on Current and Future Applications. Front Microbiol. 2021;12.

5. Imlay JA. Where in the world do bacteria experience oxidative stress? Env Micrbiol. 2019;21(2):521–30.

6. González-Flecha B, Demple B. Homeostatic regulation of intracellular hydrogen peroxide concentration in aerobically growing Escherichia coli. J Bacteriol. 1997.

7. Shvinka JE, Toma MK, Galinina NI, SkĀRds IV, Viesturs UE. Production of Superoxide Radicals during Bacterial Respiration. Microbiology. 1979;113(2):377–82.

8. Miyaji A, Suzuki M, Baba T, Kamachi T, Okura I. Hydrogen peroxide as an effecter on the inactivation of particulate methane monooxygenase under aerobic conditions. J Mol Catal B Enzym. 2009 May 1;57(1):211–5.

9. Cabiscol Català E, Tamarit Sumalla J, Ros Salvador J. Oxidative stress in bacteria and protein damage by reactive oxygen species. Intern. Micro., 2000;3(1):3-8

10. Imlay JA. The molecular mechanisms and physiological consequences of oxidative stress: lessons from a model bacterium. Nat Rev Microbiol. 2013 Jul;11(7):443–54.

11. Messner KR, Imlay JA. The identification of primary sites of superoxide and hydrogen peroxide formation in the aerobic respiratory chain and sulfite reductase complex of Escherichia coli. J Biol Chem. 1999 Apr 9;274(15):10119–28.

12. Korshunov S, Imlay JA. Two sources of endogenous H2O2 in Escherichia coli. Mol Microbiol. 2010 Mar;75(6):1389–401.

13. Ross MO, Rosenzweig AC. A tale of two methane monooxygenases. J Biol Inorg Chem. 2017 Apr 1;22(2):307–19.

14. Peng W, Qu X, Shaik S, Wang B. Deciphering the oxygen activation mechanism at the CuC site of particulate methane monooxygenase. Nat Catal. 2021 Apr;4(4):266–73.

15. Zahn J, Arciero DM, Hooper A, Coats JR, Dispirito A. Cytochrome c peroxidase from Methylococcus capsulatus Bath. Arch Microbiol. 1997 Dec;168(5):362–72.

16. Seixas AF, Quendera AP, Sousa JP, Silva AFQ, Arraiano CM, Andrade JM. Bacterial Response to Oxidative Stress and RNA Oxidation. Front Genet. 2022;12.

17. Bible AN, Khalsa-Moyers GK, Mukherjee T, Green CS, Mishra P, Purcell A, et al. Metabolic Adaptations of Azospirillum brasilense to Oxygen Stress by Cell-to-Cell Clumping and Flocculation. Appl Environ Microbiol. 2015 Dec 15;81(24):8346–57.

18. Bible A, Russell MH, Alexandre G. The Azospirillum brasilense Che1 chemotaxis pathway controls swimming velocity, which affects transient cell-to-cell clumping. J Bacteriol. 2012 Jul;194(13):3343–55.

19. Bible AN, Stephens BB, Ortega DR, Xie Z, Alexandre G. Function of a Chemotaxis-Like Signal Transduction Pathway in Modulating Motility, Cell Clumping, and Cell Length in the Alphaproteobacterium Azospirillum brasilense. J Bacteriol. 2008 Oct;190(19):6365–75.

20. Whittenbury R, Phillips KC, Wilkinson JF. Enrichment, Isolation and Some Properties of Methane-utilizing Bacteria. Microbiol. 1970;61(2):205–18.

21. Chen S, Zhou Y, Chen Y, Gu J. fastp: an ultra-fast all-in-one FASTQ preprocessor. Bioinformatics. 2018 Sep 1;34(17):i884–90.

22. Souvorov A, Agarwala R, Lipman DJ. SKESA: strategic k-mer extension for scrupulous assemblies. Genome Biol. 2018 Oct 4;19(1):153.

23. Parks DH, Imelfort M, Skennerton CT, Hugenholtz P, Tyson GW. CheckM: assessing the quality of microbial genomes recovered from isolates, single cells, and metagenomes. Genome Res. 2015 Jul;25(7):1043–55.

24. O'Leary NA, Wright MW, Brister JR, Ciufo S, Haddad D, McVeigh R, et al. Reference sequence (RefSeq) database at NCBI: current status, taxonomic expansion, and functional annotation. Nucleic Acids Res. 2016 Jan 4;44(D1):D733-745.

25. Hyatt D, Chen GL, LoCascio PF, Land ML, Larimer FW, Hauser LJ. Prodigal: prokaryotic gene recognition and translation initiation site identification. BMC Bioinformatics. 2010 Mar 8;11(1):119.

26. Seemann T. Barrnap: BAsic Rapid Ribosomal RNA Predictor. 2013.

27. Langmead B, Salzberg SL. Fast gapped-read alignment with Bowtie 2. Nat Methods. 2012 Apr;9(4):357–9.

28. Patro R, Duggal G, Love MI, Irizarry RA, Kingsford C. Salmon provides fast and bias-aware quantification of transcript expression. Nat Methods. 2017 Apr;14(4):417–9.

29. Love MI, Huber W, Anders S. Moderated estimation of fold change and dispersion for RNA-seq data with DESeq2. Genome Biol. 2014 Dec 5;15(12):550.

30. Kanehisa M, Sato Y, Morishima K. BlastKOALA and GhostKOALA: KEGG Tools for Functional Characterization of Genome and Metagenome Sequences. J Mol Biol. 2016 Feb 22;428(4):726–31.

31. Kim HJ, Graham DW. Effect of oxygen level on simultaneous nitrogenase and sMMO expression and activity in Methylosinus trichosporium OB3b and its sMMOC mutant, PP319: aerotolerant N2 fixation in PP319. FEMS Microbiol Lett. 2001 Jul 1;201(2):133–8.

32. McDonald CA, Fagan RL, Collard F, Monnier VM, Palfey BA. Oxygen Reactivity in Flavoenzymes: Context Matters. J Am Chem Soc. 2011 Oct 26;133(42):16809–11.

33. Baez A, Shiloach J. Effect of elevated oxygen concentration on bacteria, yeasts, and cells propagated for production of biological compounds. Microb Cell Fact. 2014 Dec 19;13(1):181.

34. Korshunov S, Imlay JA. Detection and quantification of superoxide formed within the periplasm of Escherichia coli. J Bacteriol. 2006 Sep;188(17):6326-34.

35. Borisov VB, Siletsky SA, Nastasi MR, Forte E. ROS Defense Systems and Terminal Oxidases in Bacteria. Antioxidants. 2021 Jun;10(6):839.

36. Guttenplan SB, Kearns DB. Regulation of flagellar motility during biofilm formation. FEMS Microbiol Revs. 2013 Nov 1;37(6):849–71.

37. Stephens BB, Loar SN, Alexandre G. Role of CheB and CheR in the Complex Chemotactic and Aerotactic Pathway of Azospirillum brasilense. J Bacteriol. 2006 Jul;188(13):4759–68.

38. Zhulin IB, Bespalov VA, Johnson MS, Taylor BL. Oxygen taxis and proton motive force in Azospirillum brasilense. J Bacteriol. 1996 Sep;178(17):5199–204.

Chapter 3

Effect of Coculturing the Methane-Oxidizing Bacterium *Methylosinus trichosporium* OB3b with *Flavobacterium*, *Cupriavidus*, or *Pseudomonas* Bacteria

Abstract

Methane-oxidizing bacteria (MOB) are critical members of methane-containing ecosystems and are highly involved in biogeochemical cycling. Despite their crucial role, there is still a lot to learn about how the MOB interact with other bacteria in their environment. This research investigates the growth conditions and community dynamics of methane-oxidizing co-cultures, focusing on the interactions between the MOB *Methylosinus trichosporium* OB3b and the non-methane-oxidizing heterotrophic bacteria (NMOHB) of the genera *Flavobacterium*, *Cupriavidus*, and *Pseudomonas*. Heterotrophic plate counts were used to determine whether NMOHB could grow in methane-oxidizing co-cultures. All three NMOHB grew in methane-oxidizing condtions suggesting carbon substrate utilization derived from methane oxidation. Furthermore, co-cultures with *Pseudomonas chlororaphis* HC exhibited enhanced methane oxidation rates compared to monoculture, indicating a stimulating effect of *P. chlororaphis* HC on methane utilization by MOB. Transcriptomic analysis revealed differential gene expression patterns in both MOB and NMOHB during co-culture and points to potential cross-feeding of C4 dicarboxylates and methanol from the MOB to the NMOHB. Further, NMOHB displayed upregulation of genes

involved in ROS remediation, suggesting a response to oxidative stress induced by methane oxidation. Additionally, NMOHB exhibited alterations in nitrogen utilization and amino acid metabolism genes, possibly reflecting adaptations to the co-culture environment. Overall, these findings shed light on the metabolic interactions between MOB and NMOHB in methane-oxidizing systems, highlighting the potential for carbon sharing, nitrogen exchange, and ROS defense mechanisms.

Introduction

Methane (CH_4) is a key greenhouse gas. It is the most abundant reduced compound in the Earth's atmosphere and its impact on the global warming effect is second only to carbon dioxide (CO_2) (1). Between geochemical and biological sources, it is estimated that 500-600 Tg of methane is introduced into the atmosphere every year and about 60% of that total is anthropogenic (2). Some of the sources of CH_4 include acrtic tundra and other wetlands, rice paddies, oceans, lakes, ponds, many different soils and sediments, landfills, and deserts. In each of these ecosystems, the major biological sink for CH_4 is oxidation to CO_2 by methane-oxidizing bacteria (MOB) (also called methanotrophs) (3). Because of their distinct role in CH_4 degradation, methanotrophs are critical components of these ecosystems and in the global carbon cycle.

Most aerobic methanotrophic bacteria are considered either type I or II methanotrophs. The most critical difference is that the type I methanotrophs utilize the ribulose monophosphate (RuMP) pathway for carbon assimilation while type II use the serine cycle (4). Prior to carbon assimilation, CH_4 is oxidized by aerobic MOB to methanol (CH_3OH) via an oxygen dependent methane monooxygenase (3). The CH_3OH is further oxidized to formaldehyde via a methanol dehydrogenase where it assimilated by either the RuMP or serine pathways (3). Remaining

formaldehyde is oxidized to formate and then to CO_2 via formaldehyde and formate dehydrogenases (3). Also, some MOB have been shown to use a complete oxidative TCA cycle (5). It has been shown that intermediate metabolites of CH_4 metabolism are released externally from the cell and made available to other organisms, including metabolites such as CH_3OH, acetate, and other organic acids (6,7).

Methanotrophs exist within microbial communities. There are several environments where CH_4 oxidizing bacteria have been described to cohabitate and be highly interactive with other members of the microbial community. Movile Cave in Romania is an underground cave system with CH_4 present in the atmosphere as well as in groundwater (8). In 2004, Hutchens et al. used a stable isotope probing method to track ^{13}C labeled CH_4 in the microbial community and discovered evidence of an active methanotrophic community, as well as cross-feeding of CH_4 derived carbon (8). These results suggest that aerobic methanotrophs actively convert CH_4 into complex organic compounds and help to sustain a diverse community of microorganisms. Similarly, in 2007, a ^{13}C labeled CH_4 experiment was carried out in rice paddy soil. It was shown that carbon derived from labeled CH_4 accumulated in a community of methanotrophs and non-methane-oxidizing heterotrophic bacteria (NMOHB) as well as amoebae, ciliates, and flagellates. This suggests that the CH_4 derived carbon can be integrated not only into the prokaryotic community but even into microeukaryotes that act as predators on the bacteria (9). CO_2 derived from microbial CH_4 oxidation has also been shown to be incorporated into in algae in peat bogs (10,11). Experiments utilizing stable isotope probing coupled with phylogenetic analyses such as these have been shown to be effective at critically analyzing carbon tracking through microbial communities (12). So, methanotrophs are critical to sustaining a variety of different ecosystems at many levels.

Some studies have been conducted to further characterize the relationships between MOB and NMOHB by analyzing which co-culture community members provide stimulatory or inhibitory growth effects for the CH_4 oxidizers in the consortia. Iguchi et al. in 2011 demonstrated that when *Methylovulum miyakonense* HT12 was grown in co-culture with one of five bacterial strains related to the genera *Rhizobium*, *Sinorhizobium*, *Mesorhizobium*, *Xanthobacter*, and *Flavobacterium,* there was a positive effect on methanotrophic growth and methane oxidation rate. Through further analysis of the stimulatory mechanism exerted by *Rhizobium* sp. Rb122, they identified cobalamin as the growth-stimulating factor. They observed this stimulatory effect for several other Gammaproteobacterial methanotrophs belonging to the genera *Methylobacter* and *Methylomonas*, but the same effect could not be observed in members of the Alphaproteobacterial methanotrophic genera *Methylocystis* and *Methylosinus* (13).

All this work established that the methane-oxidizing bacteria community is crucial to carbon cycling in a variety of environments and, at times, essential for ecosystem function and sustainability. However, there exist many questions regarding the physiological mechanisms that the microbes in CH_4 oxidizing communities use. Some work has been done detailing the specifics of the physiological, biochemical, and genetic mechanisms at work in these microbial interactions. Previous studies on the physiology of the interactions between methanotrophs and NMOHB focused on cross-feeding of CH_3OH derived from the oxidation of CH_4. In 2017, Krause et al. used a combination of transcriptomics and RT-PCR to show that CH_3OH is the dominant carbon and energy source the methanotroph *Methylobacter tundripaludum* provides to support growth of the methanol using NMOHB *Methylotenera mobilis*. They showed that in the presence of *Methylotenera mobilis*, gene expression of the MOB's dominant methanol

dehydrogenase (MDH) shifts from the lanthanide-dependent MDH (*xoxF*) to the calcium-dependent MDH (*mxaF*).

Correspondingly, CH_3OH is released into the medium only when the methanotroph expresses the MxaF-type MDH. These results suggest a cross-feeding mechanism in which the NMOHB partner induces a change in expression of methanotroph MDHs, resulting in release of methanol for its growth. This work was crucial to our understanding of the carbon transfer mechanisms at work during growth in simple MOB-NMOHB co-cultures (7). In 2019, Takeuchi et al. expanded our understanding of how MOB are affected by coculturing with NMOHB. They used RNA-seq and differential gene expression analysis of the transcriptomes of the MOB *Methylocaldum marinum* S8 and the methanol using NMOHB *Methyloceanibacter caenitepidi* Gela4 and showed that cross-feeding between the MOB and NMOHB can occur. They also showed that the NMOHB can assimilate a wide range of substrates in addition to methanol, such as acetate, ethanol, formate, and succinate when grown in co-culture with a methanotroph when CH_4 is the only available carbon source. They discovered that the expression levels of nearly half of the genes of the NMOHB were altered during co-culture growth including genes for acetyl-CoA synthesis, the ethylmalonyl-CoA (EMC) pathway, and TCA cycle that were upregulated in co-culture. Since acetyl-CoA is a starting compound of the EMC pathway and TCA cycle, compounds that can be used for the acetyl-CoA synthesis are cross-fed from the MOB to the NMOHB. They speculate that a possible source of acetyl-CoA in co-culture is acetate since expression of acetyl coenzyme A synthetase increased. Also, they showed that the MOB produced acetate (6). These studies show that CH_3OH is a possible source of carbon cross-fed in methane-oxidizing systems but not the only possible metabolite since acetate can cross-feed into NMOHB as a precursor of the EMC pathway and the TCA cycle.

These prior studies on carbon cross-feeding to NMOHB have been limited to MOB growing with other methylotrophs. This study aims to further our knowledge of carbon transfer physiology in methane-oxidizing systems by investigating how the MOB *Methylosinus trichosporium* OB3b functions in co-culture with three different NMOHB that were isolated from CH_4 oxidizing enrichment cultures, not commonly considered to be methylotrophs and are able to grow on complex growth media. These are *Flavobacterium* sp. HC, a strain of *Pseudomonas chlororaphis* HC, and a strain of *Cupriavidus* sp. HC. Each of these three bacteria are able to grow on carbon derived from CH_4 oxidation in co-culture with *M. trichosporium* OB3b, with *P. chlororaphis* HC providing a stimulatory growth effect in the system. Further transcriptomic analysis of the culture of OB3b and NMOHB indicates that some genes of the NMOHB TCA cycle as well as alcohol dehydrogenases are upregulated and that the most likely candidates for carbon utilized by NMOHB in the system are C4 dicarboxylates and CH_3OH. Also, NMOHB play a role in nitrogen cycling in the system and upregulate ROS defense genes in response to growing in co-culture with OB3b.

Methods

Growth Condition and Community Composition of Methane-Oxidizing Cocultures

Starter cultures of the NMOHB were grown statically in 100 mL of modified nitrate mineral salts (NMS) media with 0.1% peptones. The starter culture of *M. trichosporium* OB3b was grown in 100 mL of modified NMS media with 10% CH_4 in air in a 160 mL serum bottle sealed with a butyl rubber stopper.

The modified NMS medium contains (per liter of distilled water) 1 g KNO_3, 0.27 g KH_2PO_4, 1 g $MgSO_4 \cdot 7H_2O$, 0.14 g $CaCl_2 \cdot 2H_2O$, and 0.23 g Na_2HPO_4, 0.5% (v/v) acidic trace element

solution (AcTES), and 0.02% alkaline trace element solution (AlTES). AcTES contains (per liter), 2 g $FeSO_4 \cdot 7H_2O$, 0.07 g $ZnSO_4 \cdot 7H_2O$, 0.5 g $MnCl_2 \cdot 4H_2O$, 0.12 g $CoCl_2 \cdot 6H_2O$, 0.01 g $NiCl_2 \cdot 6H2O$, 0.5 g $CuSO_4$, 0.01 g H_3BO_3, 0.06 g $LaNO_3$, 0.06 g $CeNO_3$, and 100 mM HCl. The AlTES contains (per liter) 0.11 g Na_2SeO_4, 0.05 g Na_2WO_4, 0.29 g Na_2MoO_4, and 0.04 g NaOH.

Starter cultures of the co-cultures were established by adding together a stationary phase culture of one of the NMOHB, either the *Flavobacterium* sp. HC, *Pseudomonas chlororaphis* HC, or *Cupriavidus* sp. HC with a stationary phase culture of *M. trichosporium* OB3b cells in a 1:1 (v:v) ratio in modified NMS at a 1% inoculum. Cells were grown together statically in 100 mL of modified NMS media in 160 mL serum bottles with butyl rubber stoppers and a headspace gas mixture of 10% CH_4 in air. Prior to inoculation into the co-culture system, the NMOHB cells were washed 2X with modified NMS media by pelleting cells via centrifugation at 10,000 rpm for 10 minutes, discarding old media, and resuspending the cell pellet in fresh modified NMS media. Starter cultures of the co-cultures were monitored for methane depletion by gas chromatography on a Shimadzu GC-14A gas chromatograph (Shimadzu, Japan) and after 70-80% of the CH_4 was used, a 5% inoculum was transferred to 500 mL of modified NMS media in 1 L stoppered bottles in triplicate, leaving 500 mL of available gas headspace with the same headspace gas composition as the starter cultures. Newly established experimental co-cultures were incubated at 28 °C without shaking and methane depletion was measured. Methane oxidation rates (MOR) were calculated as $MOR=\ln(\Delta[CH_4])/\ln(\Delta t)$. This is the slope of the natural log of the methane depletion curve where $[CH_4]$ is the molar concentration of CH_4 and t is time elapsed in hours. Cells in each condition were harvested in late log phase by centrifugation for 20 minutes at 4 °C and 4000 X g using an Eppendorf 5910 centrifuge. The

MOR was measured and compared to *M. trichosporium* OB3b growing in monoculture under the same conditions. The co-cultures of OB3b and NMOHB, the OB3b monoculture, and each of the NMOHB grown in modified NMS media with 0.1% peptones were further subjected to transcriptomic analysis as described below. The NMOHB grown in peptones was used as a reference for how that strain may alter its growth when growing in a CH_4 oxidizing system versus with peptones.

Heterotrophic Plate Counts to Determine Growth of NMOHB in Methane-Oxidizing Cultures

Heterotrophic plate counts were used to determine if the NMOHB were growing in co-culture where only CH_4 was present as a carbon source, Cells were grown on nutrient agar (for *Pseudomonas* and *Cupriavidus*) or TSA (for *Flavobacterium*). Since these media were not incubated in the presence of CH_4, only the NMOHB were able to grow. At the point of inoculation and after 10 days of co-culture growth, 1 mL of co-culture was diluted in a tenfold dilution series, plated onto the respective solid media in triplicate and incubated at 28 °C. Colonies appearing on the media were counted after 4 days of growth. This method is visualized in **Figure 1**. These plate count data were compared to plate count data from a control where the co-culture was established as described above, but no CH_4 was added.

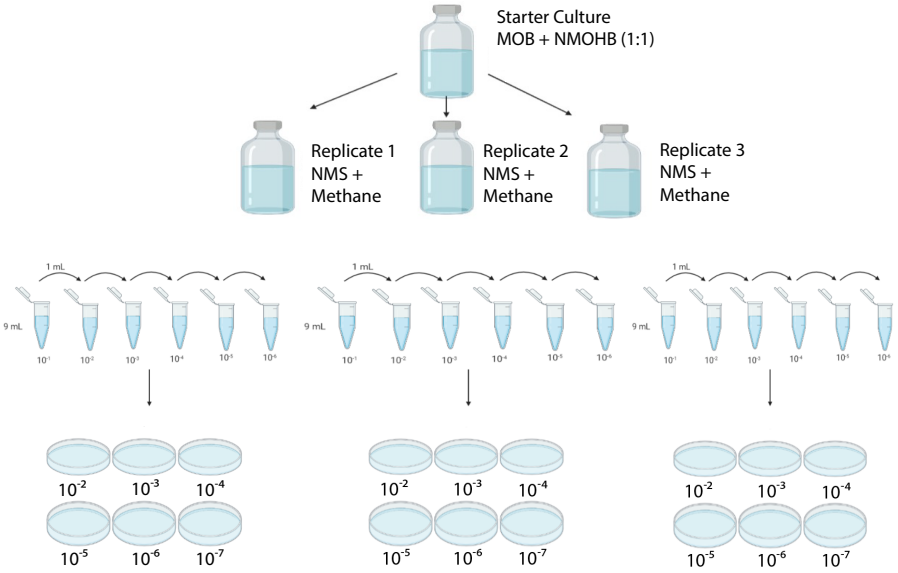

Figure 1: Visualization of the heterotrophic plate count method used to quantify the NMOHB in methane oxidizing conditions. Each replicate of NMOHB in coculture with OB3b was serially diluted and plated onto nutrient rich media in no-methane conditions and colonies were counted after 4 days of growth. This was done at the initial innoculation point and after 10 days of growth.

RNA Extraction, Illumina Library Preparation, and Sequencing

Cells for RNA extraction were grown and harvested as described above with cell pellets stored at -80 °C. The Zymo Research Quick-RNA Fungal/Bacterial Miniprep kit was used for RNA extraction. Additional DNase treatments were carried out using the Invitrogen DNase I Amplification Grade treatment kit. Nucleic acid extracts were quantified using a Qubit Fluorometer 2.0 with RNA high specificity and DNA broad range specificity reagent kits.

Illumina compatible sequencing libraries were prepared for sequencing with the Zymo-Seq RiboFree Total RNA Library Kit (Zymo Research, USA) according to the manufacturer's specifications. Prior to sequencing, the cDNA library was concentrated using a Thermo

Scientific Savant DNA120 SpeedVac Concentrator, and size selection was carried out using the Agilent 4150 TapeStation System.

Sequencing of the final cDNA library was performed at the Oklahoma Medical Research Foundation Center for Clinical Genomics (Oklahoma City, USA) using Illumina NovaSeq 6000 S4 PE150 chemistry.

Reference Genome Sequencing

Genomic DNA of *P. chlororaphis* HC from a log-phase grown culture grown in liquid TSB at 28 °C was extracted using the Qiagen DNeasy Blood and Tissue Kit. DNA was fragmented using a QSonica 800R3 sonicator and built into Illumina-compatible shotgun libraries using the KAPA HyperPrep Kit. Shotgun libraries were sequenced on an Illumina MiSeq instrument. Sequence data was processed using fastp v0.23.2 (14) to remove reads containing uncalled bases ('N'), trim low-quality bases ($q < 30$), and merge overlapping reads. The resulting analysis-ready reads were used as input for de novo assembly with SKESA v2.5.1 (15). The quality of genomes was assessed by CheckM v1.1.3 (16). The genome for *M. trichosporium* OB3b (GCF_000178815.2) was downloaded from the NCBI RefSeq database (17). Gene prediction was performed using Prodigal v2.6.3 (18) and barrnap v0.9 (19).

Read Mapping and Quantification

Raw fastq reads were filtered for high-quality reads ($q > 30$) and the adaptors were trimmed using fastp v0.22.0 (14). Quality-filtered pair-end reads were mapped to respective reference genomes using Bowtie 2 v2.2.5 (20). The .bam files generated were parsed for DNA contamination issues by removing reads known to directionally be linked to genomic DNA, then removing an equal number of reads from the RNA pool to account for bias. The pre-computed

alignments generated by Bowtie 2 were used as input for transcript quantification using Salmon 0.14.2 (21).

Differential Expression Analysis

The R program DESeq2 was used for differential expression analysis of quantified reads using the likelihood ratio test method (22). Genes that were differentially expressed (adjusted p-value < 0.05, log2FC < -2 or > 2) were annotated using KEGG BlastKOALA and differentially expressed genes in pathways were reconstructed using the KEGG Mapper Reconstruct tool (23).

Results

NMOHB Grow on Carbon Substrates Derived from Methane Oxidation by MOB

Heterotrophic plate counts on nutrient agar were used to quantify the growth of *P. chlororaphis* HC, *Cupriavidus* sp. HC, and the *Flavobacterium* sp. HC in methane-oxidizing conditions. Each of the strains were able to grow in co-culture with *M. trichosporium* OB3b on NMS medium with CH_4 as the only carbon source (**Fig. 2**). The growth of each of the NMOHB in co-culture with *M. trichosporium* OB3b was compared to a control with no added CH_4, and in this control there was no significant increase in growth, with the *Flavobacterium* species even having a slight decrease in cells over time. Each NMOHB strain was also grown in NMS and 10% CH_4 and none of the strains are able to grow on CH_4 in monoculture. This indicates that *P. chlororaphis* HC, *Cupriavidus* sp. HC, and *Flavobacterium* sp. HC are all able to grow on products produced from the oxidation of CH_4 by *M. trichosporium* OB3b.

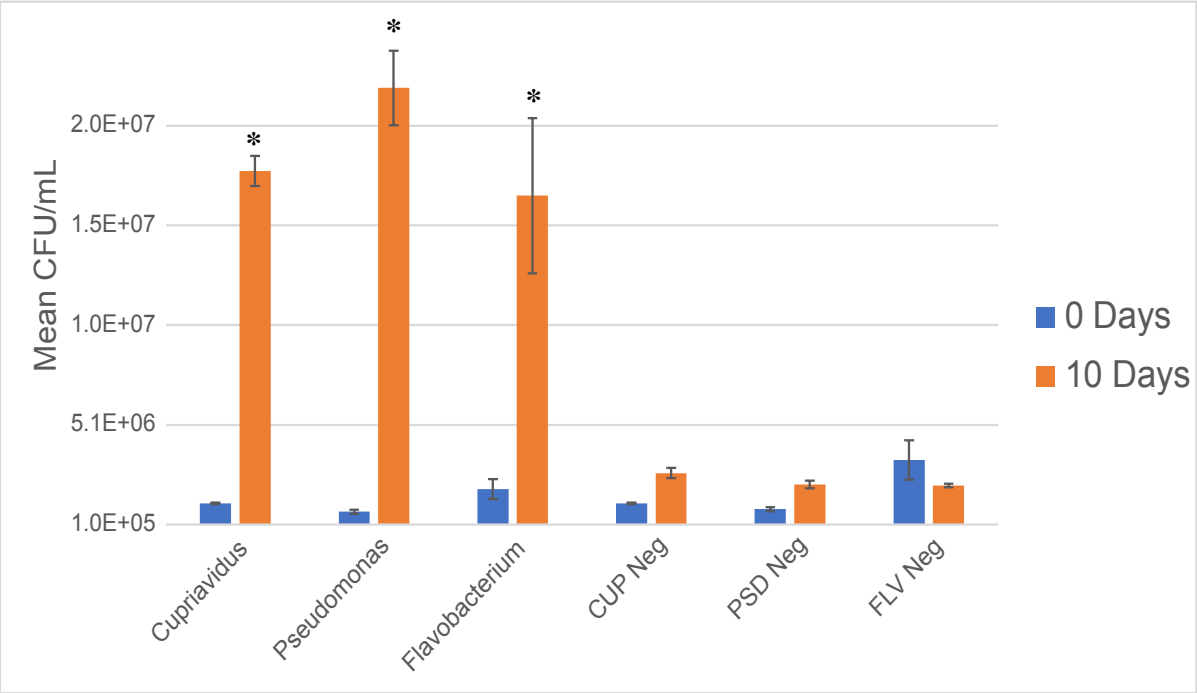

Figure 2: Mean heterotrophic plate counts (CFU/mL) of *Cupriavidus* sp. HC, *Pseudomonas chlororaphis* HC, and *Flavobacterium* sp. HC in coculture with *Methylosinus trichosporium* OB3b in methane oxiding conditions and assocated controls grown with no added methane. Error bars represent standard deviation of triplicate samples. Statistically significant differences in means (p-val < 0.05) between 0 (blue) and 10 (orange) days of growth represented by *.

The Presence of *P. chlororaphis* in Coculture with *Methylosinus trichosporium* OB3b Stimulates the Rate of Methane Oxidation

The MOR of co-cultures of either *P. chlororaphis* HC, *Cupriavidus* sp. HC, or the *Flavobacterium* sp. HC with *M. trichosporium* OB3b was measured and compared to *M. trichosporium* OB3b grown in monoculture to determine if the presence of any of the NMOHB strains stimulated the rate of CH_4 utilization by the MOB. When *M. trichosporium* OB3b is grown in co-culture with *P. chlororaphis* the MOR is greater than when *M. trichosporium* OB3b is grown in monoculture. When *M. trichosporium* OB3b is grown in co-culture with either *Cupriavidus* sp. HC or the *Flavobacterium* sp. HC, the MOR does not significantly change compared to the monoculture (**Fig. 3**). This demonstrates that the presence of *P. chlororaphis* HC, but not the other NMOHB, in culture with OB3b is stimulating the MOR of OB3b.

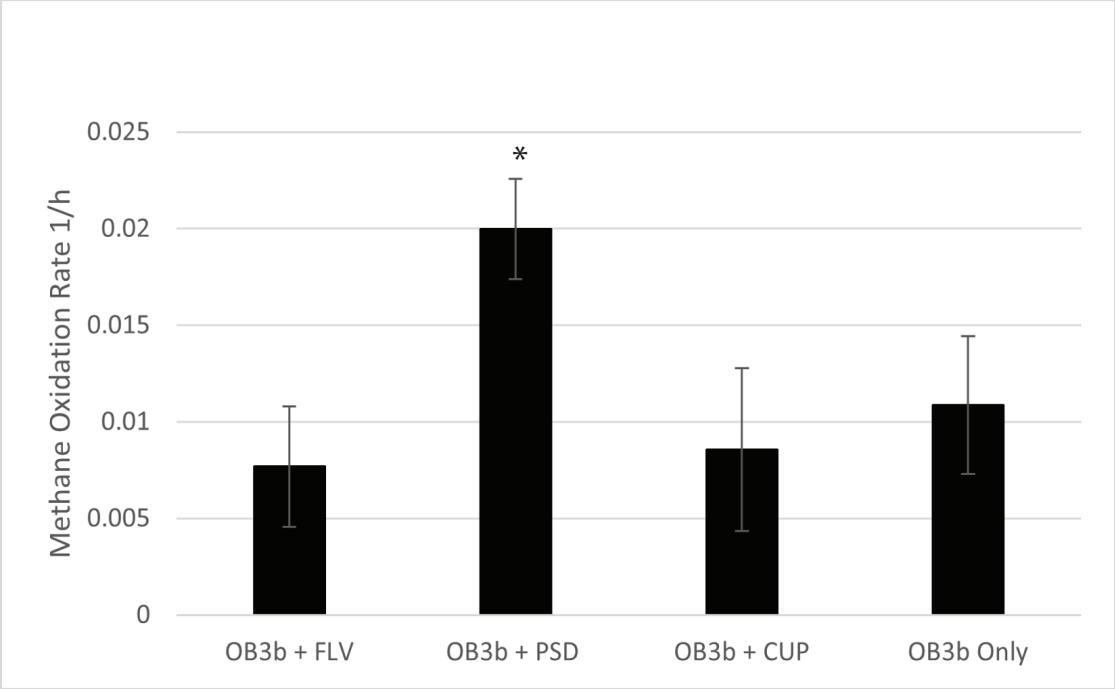

Figure 3: Mean methane oxidation rates of *Methylosinus trichosporium* OB3b in coculture with *Flavobacterium* sp. HC (FLV), *Pseudomonas chlororaphis* HC (PSD), or *Cupriavidus* sp. HC (CUP) compared to OB3b growing in monoculture. Error bars represent standard deviation of triplicate samples. There is a statistically significant (p-val < 0.05) difference in the mean methane oxidation rate of OB3b in coculture with PSD compared to OB3b in monoculture (*).

Genes Differentially Expressed by *Methylosinus trichosporium* OB3b in Coculture with NMOHB

Across all conditions, there were 25 genes, differentially expressed by *M. trichosporium* OB3b (**Table 1**). When *M. trichosporium* OB3b was in co-culture with *P. chlororaphis* HC, 20 genes were differentially expressed of which 8 were annotated. These genes included an arsenate reductase gene (*arsC*) and associated transcriptional regulators, hydroxylamine reductase (*hcp*), and the large subunit of a nitrite reductase (*nasB*). When *M. trichosporium* OB3b was in co-culture with *Cupriavidus* sp. HC, 5 genes were differentially expressed of which 4 were annotated. These included an outer membrane immunogenic protein, flavodoxin I, pyrroline-5-carboxylate reductase (*proC*), and L-ornithine Nalpha-acyltransferase (*olsB*). When *M. trichosporium* OB3b was in co-culture with *Flavobacterium* HC there were no differentially expressed genes.

Table 1: Differentially expressed genes of *Methylosinus trichosporium* OB3b in co-culture with *Pseudomonas chlororaphis* HC or *Cupriavidus* sp. HC compared to OB3b in monoculture. A negative log2FC represents genes that are expressed less in the co-culture condition. There were no differentially expressed genes in co-culture with *Flavobacterium* sp. HC.

***Methylosinus trichosporium* OB3b with *Pseudomonas chlororaphis* HC**			
Gene ID	**log2FC**	**Adj P-Value**	**Annotation**
OB3B.00001_1246	2.04	0.000693665	TC.FEV.OM; iron complex outermembrane recepter protein
OB3B.00001_1265	-2.05	0.034568834	
OB3B.00001_1283	2.90	3.52E-13	
OB3B.00001_1420	-2.24	0.003026706	TC.FEV.OM; iron complex outermembrane recepter protein
OB3B.00001_2132	-2.20	0.00240534	
OB3B.00001_2257	2.04	0.047032925	arsR; ArsR family transcriptional regulator, arsenate/arsenite/antimonite-responsive transcriptional repressor
OB3B.00001_2258	3.10	1.91E-05	
OB3B.00001_2259	3.38	0.000201778	arsC; arsenate reductase (glutaredoxin) [EC:1.20.4.1]
OB3B.00001_2260	4.30	2.11E-12	ArsD; Arsenical resistance operon trans-acting repressor
OB3B.00001_2486	3.09	2.73E-10	
OB3B.00001_249	-5.18	0.019041537	
OB3B.00001_2609	-2.68	0.001470236	
OB3B.00001_2610	9.15	0.020488634	
OB3B.00001_2936	2.36	0.044256312	hcp; hydroxylamine reductase [EC:1.7.99.1]
OB3B.00001_3242	-2.22	0.02684378	
OB3B.00001_3695	-2.00	0.003122231	parA, soj; chromosome partitioning protein
OB3B.00001_3786	-2.34	0.02192163	nasD, nasB; nitrite reductase [NAD(P)H] large subunit [EC:1.7.1.4]
OB3B.00001_3939	-3.79	0.015235756	
OB3B.00001_4109	-2.99	0.000687722	
OB3B.00001_897	2.63	0.030527272	
***Methylosinus trichosporium* OB3b with *Cupriavidus* HC**			
Gene ID	**log2FC**	**Adj P-Value**	**Annotation**
OB3B.00001_2007	-2.65286	0.005509335	
OB3B.00001_3473	-4.611125	0.004910335	omp31; outer membrane immunogenic protein
OB3B.00001_3521	3.688133	0.045081592	fldA, nifF, isiB; flavodoxin I
OB3B.00001_564	-2.863099	0.043902666	proC; pyrroline-5-carboxylate reductase [EC:1.5.1.2]
OB3B.00001_875	-4.989451	0.000324751	olsB; L-ornithine Nalpha-acyltransferase [EC:2.3.2.30]

Genes Involved in Carbon Utilization by *Cupriavidus* sp. HC

In co-culture with *M. trichosporium* OB3b, *Cupriavidus* sp. HC overexpresses *fdwB*, coding for formate dehydrogenase beta subunit as well as genes in the TCA cycle such as succinate dehydrogenase iron-sulfur subunit (*frdB*), isocitrate lyase (*aceA*), fumarate hydratase (*fumA*), and what is putatively annotated as D-malate dehydrogenase (*dmlA*). *Cupriavidus* sp. HC also shows increased expression of an alcohol dehydrogenase gene (*adh*) in co-culture with OB3b that could potentially be responsible for the utilization of methanol (**Table 2**).

Genes involved in Carbon Utilization by *Pseudomonas chlororaphis* HC

In co-culture, *P. chlororaphis* HC overexpresses an alcohol dehydrogenase gene (*alhP*) and TCA cycle genes encoding for malate dehydrogenase (*maeB*), acetyl-CoA synthetase, and fumarate hydratase (*fumC*) when compared to when *P. chlororaphis* HC growing on peptones. Additionally, a set of genes coding for an aerobic C4-dicarboxylate transport protein (*dctABD*),

is also overexpressed in co-culture with OB3b by *P. chlororaphis* HC, implying that the C4 carbon derived from the oxidation of CH_4 by OB3b could be assimilated by *P. chlororaphis* HC (**Table 2**).

Genes Involved in Carbon Utilization by *Flavobacterium* sp. HC

Flavobacterium sp. HC downregulates two genes involved in glycolysis/gluconeogenesis including glyceraldehyde 3-phosphate dehydrogenase (*gapA*) and phosphoenolpyruvate carboxykinase (*pckA*) in co-culture with OB3b compared to the monoculture. Under the same condition, it also downregulates one gene involved in the TCA cycle; succinate dehydrogenase iron-sulfur subunit (*sdhB*). Unlike in *P. chlororaphis* HC and *Cupriavidus* sp. HC, genes related to central carbon metabolism are downregulated, and there is no evidence that an alcohol dehydrogenase is being expressed in co-culture with OB3b. In light of this, it is challenging to pinpoint the pathways used for growth in co-culture with OB3b (**Table 2**).

Table 2: Differentially expressed genes related to carbon metabolism for the NMOHB in co-culture with *Methylosinus trichosporium* OB3b. A positive log2FC represents genes that are expressed more in the co-culture condition compared to the NMOHB grown in NMS + peptones medium.

Pseudomonas chlororaphis **HC with** ***Methylosinus trichosporium*** **OB3b**			
Gene ID	**log2FC**	**Adj P-Value**	**Annotation**
PCMA.00014_59	7.42736	0.03155606	*adhP* ; alcohol dehydrogenase
PCMA.00019_12	9.00466	0.031533132	*maeB* ; malate dehydrogenase
PCMA.00001_182	2.86899	0.017978906	*fumC* , fumarate hydratase, class II
PCMA.00001_49	5.83743	0.013491053	*dctA* ; aerobic C4-dicarboxylate transport protein
PCMA.00065_25	7.98401	0.017077523	*dctB* ; C4-dicarboxylate transport sensor histidine kinase
PCMA.00065_24	8.04993	0.008705995	*dctD* ;C4-dicarboxylate transport response regulator
Cupriavidus **sp HC with** ***Methylosinus trichosporium*** **OB3b**			
Gene ID	**log2FC**	**Adj P-Value**	**Annotation**
CUP.00008_11	8.08528	1.36E-05	*fdwB* ; formate dehydrogenase beta subunit
CUP.00008_60	6.77362	0.002740338	*sdhB* ; succinate dehydrogenase iron-sulfur subunit
CUP.00154_2	12.1813	0.022377965	*aceA* ; isocitrate lyase
CUP.00282_4	2.77132	0.005704623	*fumA* ; fumarate hydratase, class I
CUP.00383_2	6.44547	0.002530642	*dmlA* ; D-malate dehydrogenase
CUP.00024_14	9.61713	0.000922184	*adh* ; alcohol dehydrogenase
Flavobacterium **sp HC with** ***Methylosinus trichosporium*** **OB3b**			
Gene ID	**log2FC**	**Adj P-Value**	**Annotation**
FB1.00019_44	-4.4595	0.046665232	*gapA* ; glyceraldehyde 3-phosphate dehydrogenase
FB1.00001_337	-2.697	0.035652999	*pckA* ; phosphoenolpyruvate carboxykinase
FB1.00001_206	-2.2889	0.029635791	*sdhB* ; succinate dehydrogenase iron-sulfur subunit

Cupriavidus sp. HC Overexpresses ROS Remediation Genes in Coculture with *Methylosinus trichosporium* OB3b

When growing in co-culture with *M. trichosporium* OB3b, *Cupriavidus* sp. HC overexpresses multiple genes that could remediate toxic ROS including SOD2 Fe-Mn family superoxide dismutase, thioredoxin-dependent peroxiredoxin (*prx*), glutathione-dependent peroxiredoxin (*pgdX*), thioredoxin-dependent peroxiredoxin (*tpx*), and genes for glutathione biosynthesis from glutamate via glutamate-cysteine ligase (*gshA*) and glutathione synthase (*gshB*) which are involved in peroxide remediation (24). This implies that in co-culture with OB3b, the *Cupriavidus* sp. HC must deal with exposure to ROS by utilizing ROS remediation proteins in ways that are likely not needed when growing in NMS + Peptones (**Table 3**).

Flavobacterium HC Underexpresses ROS Remediation Genes in Coculture with *Methylosinus trichosporium* OB3b

When growing in co-culture with *M. trichosporium* OB3b, *Flavobacterium* sp. HC decreases its expression ROS remediation genes including thioredoxin 1(*trxA*), and lipoyl-dependent peroxiredoxin (*osmC*) (**Table 3**).

Pseudomonas chlororaphis Overexpresses ROS Remediation Genes in Coculture with *Methylosinus trichosporium* OB3b

When *P. chlororaphis* is growing in co-culture with *M. trichosporium* OB3b, it overexpresses genes related to the remediation of ROS species such as hydrogen peroxide and superoxide. Specifically, the strain overexpresses peroxidases including catalase (*katE*) and a thioredoxin-dependent peroxiredoxin (*prx*) (**Table 3**).

Table 3: Differentially expressed genes related to ROS remediation for the NMOHB in co-culture with *Methylosinus trichosporium* OB3b. A positive log2FC represents genes that are expressed more in the co-culture condition compared to the NMOHB grown in NMS + peptones medium.

***Pseudomonas chlororaphis* HC with *Methylosinus trichosporium* OB3b**			
Gene ID	**log2FC**	**Adj P-Value**	**Annotation**
PCMA.00077 28	3.68097	0.004639686	*katE*; catalase
PCMA.00058 20	22.5344	0.046812146	*prx*; thioredoxin-dependent peroxiredoxin
***Cupriavidus* sp HC with *Methylosinus trichosporium* OB3b**			
Gene ID	**log2FC**	**Adj P-Value**	**Annotation**
CUP.00038 5	7.62229	3.87E-02	*prx*; thioredoxin-dependent peroxiredoxin
CUP.00584 2	3.28403	6.07E-07	*tpx*; thioredoxin-dependent peroxiredoxin [EC:1.11.1.24]
CUP.00243 10	7.85164	0.017935295	gshA; glutamate--cysteine ligase
CUP.00282 4	3.63785	1.41122E-20	*gshB*; glutathione synthase [EC:6.3.2.3]
CUP.00037 2	8.84614	0.045748896	SOD2; superoxide dismutase
***Flavobacterium* sp HC with *Methylosinus trichosporium* OB3b**			
Gene ID	**log2FC**	**Adj P-Value**	**Annotation**
FB1.00019 44	-9.2792	0.00024807	*trxA*; thioredoxin 1
FB1.00004 165	-2.3608	1.057E-05	*osmC*; lipoyl-dependent peroxiredoxin

Pseudomonas chlororaphis HC Changes Expression of Nitrogen Utilization Genes Under Methane-Oxidizing Conditions

When *M. trichosporium* OB3b is growing in co-culture with *P. chlororaphis* HC, OB3b decreases its expression of the *nasBE* nitrite reductase large and small subunits. On the other hand, *P. chlororaphis* HC overexpresses the *narK* nitrate/nitrite transporter and the *nirB* nitrite reductase genes when compared to growing in NMS + peptones medium (**Table 4**), suggesting a possible shift in nitrogen metabolism in the co-culture.

Cupriavidus sp. HC Changes Expression of Nitrogen Utilization Genes Under Methane-Oxidizing Conditions

In co-culture with OB3b, *Cupriavidus* sp. HC overexpresses the nitrate/nitrite MFS transporter (*narK*), assimilatory nitrate reductase catalytic subunit (*nasA*), assimilatory nitrite reductase large subunit (*nasB*), and the assimilatory nitrite reductases large and small subunits (*nirBD*). Additionally, in co-culture with OB3b, the strain overexpresses genes related to the biosynthesis or degradation of amino acids. There is an additionally overexpressed gene related to proline degradation to glutamate via proline dehydrogenase (*putA*). It seems likely that most of these changes are in response to growing in the absence of peptones (**Table 4**).

Flavobacterium sp. HC Changes Expression of Nitrogen Utilization Genes Under Methane-Oxidizing Conditions

When *Flavobacterium* sp. HC is growing in co-culture, it overexpresses the *nrtA* and *nrtB* nitrate/nitrite transporter and transport system substrate-binding proteins. Additionally, the strain underexpresses ornithine--oxo-acid transaminase gene (*rocD*) and tryptophan synthase alpha chain gene (*trpA*), again suggesting a need for additional nitrogen (**Table 4**).

Table 4: Differentially expressed genes related to nitrogen and amino acid utilization for the NMOHB in co-culture with *Methylosinus trichosporium* OB3b. A positive log2FC represents genes that are expressed more in the co-culture condition compared to the NMOHB grown in NMS + peptones medium.

***Pseudomonas chlororaphis* HC with *Methylosinus trichosporium* OB3b**			
Gene ID	**log2FC**	**Adj P-Value**	**Annotation**
PCMA.00014_59	7.42736	0.03155606	*narK* ; nitrate/nitrite transporter
PCMA.00045_11	12.3807	0.025245203	*nirB;* nitrite reductase
***Cupriavidus* sp HC with *Methylosinus trichosporium* OB3b**			
Gene ID	**log2FC**	**Adj P-Value**	**Annotation**
CUP.00164_7	8.80157	0.001428358	*narK* ; nitrate/nitrite transporter
CUP.00164_10	2.9744	0.039483739	*nasB* ; nitrite reductase [NAD(P)H] large subunit
CUP.00164_11	3.14536	0.000405005	*nasA* ; assimilatory nitrate reductase catalytic subunit
CUP.00164_8	8.86943	0.007747264	*nirB* ; nitrite reductase (NADH) large subunit [EC:1.7.1.15]
CUP.00164_9	6.03439	0.014278022	*nirD* ; nitrite reductase (NADH) small subunit [EC:1.7.1.15]
CUP.00467_1	3.14531	0.048500913	*putA* ; proline dehydrogenase
***Flavobacterium* sp HC with *Methylosinus trichosporium* OB3b**			
Gene ID	**log2FC**	**Adj P-Value**	**Annotation**
FB1.00001_16	2.0401	0.032168366	*nrtA* ; nitrate/nitrite transport system substrate-binding protein
FB1.00001_17	2.10538	0.000780906	*nrtB* ; nitrate/nitrite transport system substrate-binding protein
FB1.00004_84	-2.0899	0.000398162	*rocD* ;ornithine--oxo-acid transaminase
FB1.00005_80	-6.7143	0.017739174	*trpA* ; tryptophan synthase alpha chain

Discussion

Cross-feeding of Methane Derived Carbon to NMOHB in Coculture Conditions

This study shows potential ways that carbon sharing occurs between OB3b and *P. chlororaphis* HC by observing the transcription of genes related to metabolism of metabolites that could be derived from CH_4 oxidation such as methanol and C4 dicarboxylates. This study indicates that *P. chlororaphis* HC and *Cupriavidus* sp. HC express alcohol dehydrogenases that could potentially be expressed to oxidize methanol derived from the initial step of CH_4 oxidation to methanol by methane monooxygenase in OB3b. It has been shown that in strict methylotrophs, methanol cross-feeding can occur and that the non-methane-oxidizing strains can even cause the MOB to shift expression of methanol dehydrogenase from a high affinity methanol dehydrogenase (MDh) to a low affinity MDh, thereby facilitating the release of methanol by the MOB cells for use by the non-methane-oxidizing bacteria (7). OB3b expresses both the high affinity *xoxF* and low affinity *mxaF* type MDhs in co-culture with each of the NMOHB and in monoculture, but there is no indication that OB3b switches expression to the low affinity MDh in co-culture. But because expression of the *mxaF* type is essential in some MOB for release of methanol from the cell in other MOB such as in the system studied by Krause et al. (7), it is reasonable that some methanol would be accessible to the NMOHB.

It is likely the *P. chlororaphis* HC strain may also be taking up TCA cycle intermediates including fumarate, succinate, or malate derived from CH_4 oxidation. This carbon could be assimilated by *P. chlororaphis* HC via the *dctABD* C4 dicarboxylate transport system which is expressed by *P. chlororaphis* HC in co-culture with OB3b and would correlate with the observation that fumarate hydratase and malate dehydrogenase are overexpressed by *P.*

chlororaphis HC. The expression of the transporter gene *dctA* is critical to the use of C4 carbon by *P. chlororaphis*. Other studies have shown that in *Pseudomonas chlororaphis* strain O6, the expression of *dctA* is directly linked to its utilization of C4 dicarboxylate carbon utilized in the TCA cycle and mutants of strain O6 lacking in their ability to expresses the *dctA* transport gene do not grow on succinate or fumarate and show reduced growth on malate (25–28). This demonstrates the potential for cross-feeding of carbon in methane-oxidizing systems is not necessarily strictly limited to methanol in this system, and perhaps C4 substrates such as fumarate, succinate, or malate are being directly fed into the TCA cycle. There is no indication that transport of C4 substrates is upregulated, however a number of TCA cycle genes in *Cupriavidus* sp. HC were also upregulated indicating a similar type of interaction within the *Cupriavidis* and *Pseudomonas* co-cultures.

NMOHB Expression of Nitrogen Utilization Genes in Methane-Oxidizing Conditions

A likely reason that *Cupriavidus* sp. HC may be increasing its expression of the proline dehydrogenase (*putA)* gene involved in the degradation of proline to glutamate in co-culture with OB3b could be that there is simply a shift in the types of amino acids available for metabolism when changing from growth in media with peptones to growth in a CH_4 oxidizing system. It is also observed that OB3b is downregulating *proC,* which catalyzes the biosynthesis of proline, this may also be a response to changing levels of proline available in the co-culture system compared to the monoculture system. While with these data it is hard to pinpoint the specific interactions and amino acid flux across conditions, the data suggest the cross-feeding of amino acids. It has been previously shown that bacterial community structure impacts the available amino acids in a given environment and cross-feeding of amino acids is a prominent interaction of bacterial co-cultures (29,30).

Also of note is that the upregulation of nitrate/nitrite transport system genes occurs in all NMOHB when in co-culture with OB3b. Expression of these genes is essential to the transport of nitrogen anions (31) and may be an indicator of nitrogen anion exchange in the co-culture system; however, the precise mechanism of exchange is unknown. Also of note is that OB3b decreases its expression of *nasBE,* the assimilatory nitrite reductase large and small subunits when in co-culture with *P. chlororaphis* HC while *P. chlororaphis* HC increases expression of the soluble nitrite reductase *nirB* in the same condition. Though with these data alone, it is challenging to elucidate the exact role of each organism in the nitrite metabolism, it has been demonstrated that bacteria within microbial biofilms may cooperate in ways such that aerobic methanotrophs and heterotrophic denitrifiers couple oxidation of methane or methane intermediates with denitrification (32). Since the *nas* genes encoding for assimilatory nitrite reduction in OB3b are being downregulated in co-culture, and *nir* (nitrite reductase) is being overexpressed by *P. chlororaphis* HC in the same condition, perhaps *P. chlororaphis* HC is using electrons from the oxidation of CH_4 derived metabolites to reduce nitrite in the methane-oxidizing system.

NMOHB May Need to Compensate for the Buildup of Toxic ROS When Growing with OB3b

Each of the NMOHB express ROS defense genes in co-culture with OB3b more than they do when growing in monoculture in NMS + peptones medium. It appears that *P. chlororaphis* HC deals with the effects of growing in co-culture with MOB in a methane-oxidizing system by expressing catalase (*katE*), and thioredoxin-dependent peroxiredoxin (*prx*). *Cupriavidus* sp. HC also overexpresses the SOD2 Fe-Mn family superoxide dismutase in co-culture, as well as thioredoxin-dependent peroxiredoxin (*prx*). But it also overexpresses glutathione-dependent

peroxiredoxin (*pgdX*), and thioredoxin-dependent peroxiredoxin (*tpx*) and genes for glutathione biosynthesis from glutamate via glutamate-cysteine ligase (*gshA*) and glutathione synthase (*gshB*). Unlike the other two strains, *Flavobacterium* actually decreases its expression of the ROS genes thioredoxin 1(*trxA*) and lipoyl-dependent peroxiredoxin (*osmC*) in co-culture with OB3b. While OB3b possesses and is expressing in monoculture and co-culture conditions several genes related to ROS remediation such as SOD2 superoxide dismutase, catalase peroxidase (*katG*), these genes are not being differentially expressed across conditions.

During aerobic metabolism toxic reactive oxygen species (ROS) are generated including superoxide and hydrogen peroxide. (33–37). This endogenous production of ROS can have harmful effects on cells including damaging proteins, nucleic acids, and lipids (37). In addition to potential generation of toxic ROS by cellular respiration, aerobic MOB oxidize methane using methane monooxygenases that catalyze the oxidation of methane to methanol in the presence of dioxygen that may contribute to ROS generation (38). Bacteria possess a wide variety of ROS defense mechanisms including the expression of genes that code for proteins that directly act on ROS to reduce toxic effects. Some of the genes responsible for ROS remediation are being expressed by NMOHB in co-culture with OB3b including catalase (37), SOD (39), thioredoxin-dependent peroxiredoxin (40), thioredoxin 1, and lipoyl-dependent peroxiredoxin (40). When NMOHB shift from growing in peptones to growing on carbon derived from methane oxidation, they seem to alter the way that they deal with ROS by overexpressing certain ROS genes. There were some similarities in that the *P. chlororaphis* HC and *Cupriavidus* sp. HC both overexpressed *prx* genes when growing in co-culture. The observation that *Cupriavidus* sp. HC overexpresses genes for glutathione biosynthesis from glutamate via glutamate-cysteine ligase (*gshA*) and glutathione synthase (*gshB*) as a response to stress from peroxide exposure has also

been demonstrated in strains of *Pseudomonas aeruginosa*, where the *gshA* and *gshB* genes are overexpressed in response to different peroxides introduced into the growth system (24). In general, NMOHB appear to upregulate ROS defense genes as a response to growing in methane-oxidizing conditions compared to growing on peptones, however *Flavobacterium* sp. HC downregulates theses genes in co-culture pointing to the variation of ROS response across organisms.

Conclusion

The NMOHB *Pseudomonas chlororaphis* HC, *Cupriavidus* sp. HC, and *Flavobacterium* sp. HC all grow in methane-oxidizing conditions when in co-culture with *Methylosinus trichosporium* OB3b and that co-cultures of *P. chlororaphis* HC and *M. trichosporium* OB3b present increased MOR compared to OB3b growing in monoculture. Transcriptomics analysis reveals that carbon sharing between OB3b and the NMOHB is most likely occurring as cross-feeding of methanol and/or C4 dicarboxylates. Also, nitrite and amino acid metabolism are altered in both OB3b and NMOHB when growing in co-culture and ROS defense genes by NMOHB are differentially expressed during growth in co-culture with OB3b. These observations provide insight into how NMOHB that are not strict methylotrophs respond to growth in methane-oxidizing systems.

References

1. Dean JF, Middelburg JJ, Röckmann T, Aerts R, Blauw LG, Egger M, et al. Methane Feedbacks to the Global Climate System in a Warmer World. Rev of Geophys. 2018;56(1):207–50.

2. Saunois M, Stavert AR, Poulter B, Bousquet P, Canadell JG, Jackson RB, et al. The Global Methane Budget 2000–2017. Earth Syst Sci Data. 2020 Jul 15;12(3):1561–623.

3. Hanson RS, Hanson TE. Methanotrophic bacteria. Microbiol Rev. 1996 Jun;60(2):439–71.

4. Bowman, J. (2006). The Methanotrophs — The Families Methylococcaceae and Methylocystaceae. In: Dworkin, M., Falkow, S., Rosenberg, E., Schleifer, KH., Stackebrandt, E. (eds) The Prokaryotes. Springer, New York, NY. https://doi.org/10.1007/0-387-30745-1_15

5. Fu Y, Li Y, Lidstrom M. The oxidative TCA cycle operates during methanotrophic growth of the Type I methanotroph Methylomicrobium buryatense 5GB1. Metab Eng. 2017 Jul 1;42:43–51.

6. Takeuchi M, Ozaki H, Hiraoka S, Kamagata Y, Sakata S, Yoshioka H, et al. Possible cross-feeding pathway of facultative methylotroph Methyloceanibacter caenitepidi Gela4 on methanotroph Methylocaldum marinum S8. PLOS ONE. 2019 Mar 14;14(3):e0213535.

7. Krause SMB, Johnson T, Samadhi Karunaratne Y, Fu Y, Beck DAC, Chistoserdova L, et al. Lanthanide-dependent cross-feeding of methane-derived carbon is linked by microbial community interactions. Proc Natl Acad Sci USA. 2017 Jan 10;114(2):358–63.

8. Hutchens E, Radajewski S, Dumont MG, McDonald IR, Murrell JC. Analysis of methanotrophic bacteria in Movile Cave by stable isotope probing. Environ Microbiol. 2004;6(2):111–20.

9. Murase J, Frenzel P. A methane-driven microbial food web in a wetland rice soil. Environ Microbiol. 2007;9(12):3025–34.

10. Raghoebarsing AA, Smolders AJP, Schmid MC, Rijpstra WIC, Wolters-Arts M, Derksen J, et al. Methanotrophic symbionts provide carbon for photosynthesis in peat bogs. Nature. 2005 Aug;436(7054):1153–6.

11. van Duinen GA, Vermonden K, Bodelier PLE, Hendriks AJ, Leuven RSEW, Middelburg JJ, et al. Methane as a carbon source for the food web in raised bog pools. Freshwater Sci. 2013 Dec;32(4):1260–72.

12. McDonald IR, Radajewski S, Murrell JC. Stable isotope probing of nucleic acids in methanotrophs and methylotrophs: A review. Org Geochem. 2005 May;36(5):779–87.

13. Iguchi H, Yurimoto H, Sakai Y. Stimulation of Methanotrophic Growth in Cocultures by Cobalamin Excreted by Rhizobia. App Environ Microbiol. 2011 Dec 15;77(24):8509–15.

14. Chen S, Zhou Y, Chen Y, Gu J. fastp: an ultra-fast all-in-one FASTQ preprocessor. Bioinformatics. 2018 Sep 1;34(17):i884–90.

15. Souvorov A, Agarwala R, Lipman DJ. SKESA: strategic k-mer extension for scrupulous assemblies. Genome Biol. 2018 Oct 4;19(1):153.

16. Parks DH, Imelfort M, Skennerton CT, Hugenholtz P, Tyson GW. CheckM: assessing the quality of microbial genomes recovered from isolates, single cells, and metagenomes. Genome Res. 2015 Jul;25(7):1043–55.

17. O'Leary NA, Wright MW, Brister JR, Ciufo S, Haddad D, McVeigh R, et al. Reference sequence (RefSeq) database at NCBI: current status, taxonomic expansion, and functional annotation. Nucleic Acids Res. 2016 Jan 4;44(D1):D733-745.

18. Hyatt D, Chen GL, LoCascio PF, Land ML, Larimer FW, Hauser LJ. Prodigal: prokaryotic gene recognition and translation initiation site identification. BMC Bioinformatics. 2010 Mar 8;11(1):119.

19. Seemann T. Barrnap: BAsic Rapid Ribosomal RNA Predictor. 2013.

20. Langmead B, Salzberg SL. Fast gapped-read alignment with Bowtie 2. Nat Methods. 2012 Apr;9(4):357–9.

21. Patro R, Duggal G, Love MI, Irizarry RA, Kingsford C. Salmon provides fast and bias-aware quantification of transcript expression. Nat Methods. 2017 Apr;14(4):417–9.

22. Love MI, Huber W, Anders S. Moderated estimation of fold change and dispersion for RNA-seq data with DESeq2. Genome Biol. 2014 Dec 5;15(12):550.

23. Kanehisa M, Sato Y, Morishima K. BlastKOALA and GhostKOALA: KEGG Tools for Functional Characterization of Genome and Metagenome Sequences. J Mol Bio. 2016 Feb 22;428(4):726–31.

24. Wongsaroj L, Saninjuk K, Romsang A, Duang-nkern J, Trinachartvanit W, Vattanaviboon P, et al. Pseudomonas aeruginosa glutathione biosynthesis genes play multiple roles in stress protection, bacterial virulence and biofilm formation. PLOS ONE. 2018 Oct 16;13(10):e0205815.

25. Valentini M, Storelli N, Lapouge K. Identification of C4-Dicarboxylate Transport Systems in Pseudomonas aeruginosa PAO1. J Bacteriol. 2011 Sep;193(17):4307–16.

26. Forward JA, Behrendt MC, Wyborn NR, Cross R, Kelly DJ. TRAP transporters: a new family of periplasmic solute transport systems encoded by the dctPQM genes of Rhodobacter capsulatus and by homologs in diverse gram-negative bacteria. J Bacteriol. 1997 Sep;179(17):5482–93.

27. Nam HS, Anderson AJ, Yang KY, Cho BH, Kim YC. The dctA gene of Pseudomonas chlororaphis O6 is under RpoN control and is required for effective root colonization and induction of systemic resistance. FEMS Microbiol Letts. 2006 Mar 1;256(1):98–104.

28. Youn JW, Jolkver E, Krämer R, Marin K, Wendisch VF. Characterization of the Dicarboxylate Transporter DctA in Corynebacterium glutamicum. J Bacteriol. 2009 Sep;191(17):5480–8.

29. Du J, Yin Q, Zhou X, Guo Q, Wu G. Distribution of extracellular amino acids and their potential functions in microbial cross-feeding in anaerobic digestion systems. Bioresour Technol. 2022 Sep 1;360:127535.

30. Ecology and evolution of metabolic cross-feeding interactions in bacteria. Nat Prod Rep. 2018 Jan 1;35(5):455–88.

31. Noji S, Nohno T, Saito T, Taniguchi S. The narK gene product participates in nitrate transport induced in Escherichia coli nitrate-respiring cells. FEBS Letters. 1989;252(1–2):139–43.

32. Lee J, Alrashed W, Engel K, Yoo K, Neufeld JD, Lee HS. Methane-based denitrification kinetics and syntrophy in a membrane biofilm reactor at low methane pressure. Sci Total Environ. 2019 Dec 10;695:133818.

33. Imlay JA. Where in the world do bacteria experience oxidative stress? Environ Microbiol. 2019;21(2):521–30.

34. González-Flecha B, Demple B. Homeostatic regulation of intracellular hydrogen peroxide concentration in aerobically growing Escherichia coli. J Bacteriol. 1997

35. Shvinka JE, Toma MK, Galinina NI, SkĀRds IV, Viesturs UE. Production of Superoxide Radicals during Bacterial Respiration. Microbiol. 1979;113(2):377–82.

36. Miyaji A, Suzuki M, Baba T, Kamachi T, Okura I. Hydrogen peroxide as an effecter on the inactivation of particulate methane monooxygenase under aerobic conditions. J Mol Catal B: Enzym. 2009 May 1;57(1):211–5.

37. Cabiscol Català E, Tamarit Sumalla J, Ros Salvador J. Oxidative stress in bacteria and protein damage by reactive oxygen species. Intern. Micro., 2000;3(1):3-8

38. Ross MO, Rosenzweig AC. A tale of two methane monooxygenases. J Biol Inorg Chem. 2017 Apr 1;22(2):307–19.

39. Imlay JA. The molecular mechanisms and physiological consequences of oxidative stress: lessons from a model bacterium. Nat Rev Microbiol. 2013 Jul;11(7):443–54.

40. Lu J, Holmgren A. The thioredoxin antioxidant system. Free Radic Biol Med. 2014 Jan;66:75–87.

Chapter 4

Conclusion

The whole of the work present in the previous chapters demonstrates the breadth and diversity of research regarding our understanding of the group of organisms known as methane-oxidizing bacteria. The research is this field is so diverse because the impact of these organisms is critical to the carbon flux in a very wide variety of ecosystems, and methane metabolism is often the focus of many biotechnological applications including the generation of value-added products, and remediation of pollutants.

This work summarized the knowledge gaps in the fields of ecology and physiology of methane-oxidizing bacteria including how there was a lack of research into how different concentrations of oxygen or the presence of catalase in growth media as an ROS scavenger may affect the methane oxidation rate and alter the expression of ROS defense genes in MOB. This was despite previous knowledge of the chemical potential for MOB to generate ROS during methane metabolism and the critical role that oxygen flux and balance has on the physiology of any organism. This study demonstrates for the first time that methane-oxidizing bacteria alter their expression of ROS defense genes as a physiological response to increases in oxygen concentration and that some MOB such as *Methylomonas* sp. WSC-7 may even utilize cell clumping as a response to unfavorable oxygen conditions. There are several implications to these findings. Foremost, it should be noted that even given that only two MOB were discussed at depth during our investigation into how oxygen impacts MOB physiology, there were major distinctions. Properly understanding and optimizing oxygen concentrations is critical when trying to utilize the unique abilities of methane oxidizers for biotechnological and bioremediation

purposes. Further, as researchers aim to isolate and characterize more methane oxidizers, careful consideration should be made to how ROS generation may hinder our ability to do so effectively. Consideration of oxygen concentrations in the environments where MOB are isolated should be paramount, as unfavorable oxygen concentrations could potentially lead to decreases in methane metabolism, and certain MOB being outcompeted during the enrichment process by MOB that have a wide variety of means allowing them to scavenge ROS and not be adversely affected by ROS toxicity. To further our understanding of how ROS and changes in oxygen concentration impact MOB, it would be beneficial to understand MOB response across a wider range of MOB and try to correlate physiological response to ROS with MOB ecology and evolution. This would allow for more precise means of refining enrichment conditions for the targeted isolation of a wider variety of MOB.

In addition to presenting a refined overview of how MOB respond to changes in oxygen concentration, this work also presented a novel perspective of how MOB behave in co-culture with a variety of NMOHB that were isolated from methane-oxidizing enrichment cultures. This work helped identify some potential means of carbon flux in our established co-culture systems, and also demonstrated that NMOHB express ROS defense genes when growing in methane-oxidizing systems. Until now, most work done on how MOB and NMOHB interact in co-culture had been limited to carbon flux and cross-feeding. This work helped pinpoint potential modes of cross-feeding in our system, and also expanded the understanding of MOB community interactions by demonstrating the potential for NMOHB to deal with the negative consequences of ROS in co-culture, that there are changes in the expression of nitrite and amino acid utilization genes. It has been established that in some cases, the presence of NMOHB in co-culture with MOB can provide growth stimulating effects to the MOB leading to increased growth rates or

MOR rates in these systems. Further, this work shows that when *Methylosinus trichosporium* OB3b is in co-culture with *Pseudomonas chlororaphis* HC there is a growth stimulating effect. However, the cause of his stimulation of the MOR is unknown. Some future directions for this work may include trying to identify how MOB and NMOHB from the same ecosystem interreact to give insight into more ecologically relevant findings. This study utilized NMOHB that were isolated from methane-oxidizing enrichment cultures, but they may not primarily rely on methane-derived carbon in the natural environment, nor is it assumed that they coexist with species of *Methylosinus*.

Finally, this dissertation presents the isolation and characterization of a novel species of MOB, *Methylocystis suflitae*, named for University of Oklahoma emeritus professor Joseph M. Suflita. The characterization of this species highlights a critical aspect of research in the study of MOB, but also in microbiology research as well. Successful discovery and taxonomic classification of new species of microorganisms is an essential component to understanding microbial ecology and cultivating new organisms for the use of microbes to better our world through biotechnological applications. In light of the other work presented in this dissertation, I am hopeful that considerations regarding oxygen concentration, and how microbes are interacting in their broader community may help to refine methods of enrichment and isolation of novel bacteria, especially in targeted approaches following the identification of the presence of specific microorganisms within a particular environment by metagenomic, functional gene, or 16S rRNA surveys.